



Published in final edited form as:

J Med Chem. 2022 January 13; 65(1): 303–322. doi:10.1021/acs.jmedchem.1c01473.

Structure-Activity Relationship Study of Subtype-Selective Positive Modulators of K_{Ca2} Channels

Naglaa Salem El-Sayed^{†, #}, Young-Woo Nam^{†, #}, Polina A Egorova^{‡, #}, Hai Minh Nguyen[§], Razan Orfali[†], Mohammad Asikur Rahman[†], Grace Yang[†], Heike Wulff[§], Ilya Bezprozvanny^{*, ‡, //}, Keykavous Parang^{*, †}, Miao Zhang^{*, †}

[†]Department of Biomedical and Pharmaceutical Sciences, Chapman University School of Pharmacy, 9401 Jeronimo Road, Irvine, CA 92618, USA

[‡]Laboratory of Molecular Neurodegeneration, Peter the Great St. Petersburg Polytechnic University, Politekhnikeskaya Ulitsa, 29, St. Petersburg, 195251, Russia

[§]Department of Pharmacology, School of Medicine, University of California, Davis, 451 Health Sciences Drive, Davis, CA 95616, USA

^{//}Department of Physiology, University of Texas Southwestern Medical Center, 6001 Forest Park Road, Dallas, TX 75390, USA

Abstract

A series of modified *N*-cyclohexyl-2-(3,5-dimethyl-1*H*-pyrazol-1-yl)-6-methylpyrimidin-4-amine (CyPPA) analogs were synthesized by replacing the cyclohexane moiety with different 4-substituted cyclohexane rings, tyrosine analogs, or mono- and dihalophenyl rings, and were subsequently studied for their potentiation of K_{Ca2} channel activity. Among the *N*-benzene-*N*-[2-(3,5-dimethyl-pyrazol-1-yl)-6-methyl-4-pyrimidinamine derivatives, halogen decoration at positions 2 and 5 of benzene-substituted 4-pyrimidineamine in compound **2q** conferred ~10-fold higher potency, while halogen substitution at positions 3 and 4 of benzene-substituted 4-pyrimidineamine in compound **2o** conferred ~7-fold higher potency on potentiating $K_{Ca2.2a}$

***Corresponding Author: Ilya Bezprozvanny** - Department of Physiology, University of Texas Southwestern Medical Center, 6001 Forest Park Road, Dallas, TX 75390, USA; Laboratory of Molecular Neurodegeneration, Peter the Great St. Petersburg Polytechnic University, Politekhnikeskaya Ulitsa, 29, St. Petersburg, Russia. Tel: +1-214-645-6017; ilya.bezprozvanny@utsouthwestern.edu; **Keykavous Parang** - Department of Biomedical and Pharmaceutical Sciences, Chapman University School of Pharmacy, 9501 Jeronimo Road, Irvine, CA 92618, USA, Tel: +1-714-516-5489; Fax: +1-714-516-5481; parang@chapman.edu; **Miao Zhang** - Department of Biomedical and Pharmaceutical Sciences, Chapman University School of Pharmacy, 9501 Jeronimo Road, Irvine, CA 92618, USA, Tel: +1-714-516-5478; Fax: +1-714-516-5481; zhang@chapman.edu.

[#]N.S.E., Y.W.N. and P.A.E. contributed equally to this work.

Author Contributions

N.S.E. undertook chemical synthesis. Y.W.N. and G.Y. undertook molecular biology and cell culture studies. Y.W.N., R.O., M.A.R. and M.Z. undertook *in vitro* electrophysiology studies of $K_{Ca2.x}/K_{Ca3.1}$ channels. H.M.N. and H.W. undertook *in vitro* electrophysiology studies of $K_{Ca1.1}$ and $Na_v1.2$ channels. P.A.E. undertook *ex vivo* electrophysiology studies. K.P. supervised the synthesis and structure-activity relationship studies. M.Z., N.S., I.B. and K.P. wrote the manuscript. All authors contributed to the Figures. All authors have read and agreed to the published version of the manuscript.

Naglaa Salem El-Sayed - Current address: Cellulose and Paper Department, National Research Center, 33 El-Bouhos St. (former Tahrir St.), Dokki, Giza, Egypt, P.O.X 12622

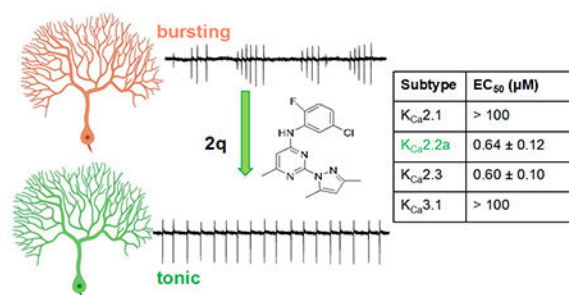
Supporting Information

¹H NMR, ¹³C NMR, and representative HPLC profiles of the compounds are provided. Molecular Formula Strings are included. Supporting information is available free of charge via the Internet at <http://pubs.acs.org>.

The authors declare no conflict of interest.

channels, compared to the parent template CyPPA. Both compounds retained the $K_{Ca2.2a}/K_{Ca2.3}$ subtype selectivity. Based on the initial evaluation, compounds **2o** and **2q** were selected for testing in an electrophysiological model of spinocerebellar ataxia type 2 (SCA2). Both compounds were able to normalize abnormal firing of Purkinje cells in cerebellar slices from SCA2 mice, suggesting the potential therapeutic usefulness of these compounds for treating symptoms of ataxia.

Graphical Abstract



Keywords

chemical synthesis; ion channel; patch-clamp; positive modulator; cerebellum; ataxia

1. INTRODUCTION

Small-conductance Ca^{2+} -activated K^+ (K_{Ca2} or SK) channels have emerged as one of the principal ion channels involved in the pacemaking of cerebellar Purkinje cells (PCs)¹. Cerebellar PCs are the primary locus of the pathology of spinocerebellar ataxia (SCA)^{2, 3}. There are four mammalian genes identified in the *KCNN* family, including *KCNN1* encoding $K_{Ca2.1}$ (SK1), *KCNN2* encoding $K_{Ca2.2}$ (SK2), *KCNN3* encoding $K_{Ca2.3}$ (SK3), and *KCNN4* encoding $K_{Ca3.1}$ (SK4, IK) channels, respectively⁴. Among the $K_{Ca2.x}/K_{Ca3.1}$ channel subtypes, $K_{Ca2.2}$ is the predominant subtype that is expressed in the cerebellum⁵⁻⁷. Loss-of-function mutations that diminish $K_{Ca2.2}$ channel activity have been linked with tremor and ataxia symptoms in rodents⁸ and humans^{9, 10}.

For decades, significant efforts have been devoted to the development of subtype-selective positive modulators of K_{Ca2} channels. The prototype subtype-selective positive modulator CyPPA has been previously reported to potentiate the $K_{Ca2.2}$ and $K_{Ca2.3}$, but not the $K_{Ca2.1}$ and $K_{Ca3.1}$ channel subtypes¹¹. The low potency of CyPPA in the micromolar range makes it unfit for clinical use. Recently, the structure of human $K_{Ca3.1}$ channels has been determined by cryogenic-electron microscopy (cryo-EM)¹². These full-length structures, including the transmembrane domains are better tools for structure-aided drug discovery than the crystal structure of the cytoplasmic domain¹³.

We generated a homology model of the $K_{Ca2.2a}$ channel using the $K_{Ca3.1}$ channel cryo-EM structure in the presence of Ca^{2+} (PDB: 6cnn)¹⁴. The K_{Ca2} channels can form homotetramers in complex with four of the Ca^{2+} -binding protein calmodulin (CaM). The

C-lobe of CaM is associated with the channel alpha subunits at the HA/HB helices. With combined computational, site-directed mutagenesis and electrophysiology approaches, we identified a pocket for CyPPA between the HA/HB helices and the C-lobe of CaM¹⁵.

After elucidating the CyPPA-channel interactions from the perspective of the drug target, here we discuss the synthesis and evaluation of a new series of CyPPA analogs. Considering the largely hydrophobic nature of the pocket between the CaM C-lobe and the HA/HB helices¹⁵, we evaluated the impact of replacing the cyclohexane moiety in CyPPA with different 4-substituted cyclohexyl rings, tyrosine analogs, mono and dihalogen and other substituted phenyl rings. Changing the position of the attached pyrazole and replacing it with an oxazolyl or imidazolyl ring, as well as substitutions of the pyrimidine ring with a pyridazine ring were also studied. A number of newly developed compounds demonstrated the ability to potentiate activity of K_{Ca2.2a} channels while retaining the K_{Ca2.2a}/K_{Ca2.3} subtype selectivity, and to normalize firing of cerebellar PCs in the model of spinocerebellar ataxia type 2 (SCA2).

2. RESULTS AND DISCUSSION

2.1. Chemistry

The chemical structure of the template, CyPPA is shown in Table 1. Scheme 1 depicts the synthesis of 4-aminosubstituted analogs of 2-(3,5-dimethyl-1*H*-pyrazol-1-yl)-6-methylpyrimidine (**2a-f**) using 4-substituted cyclohexan-1-amine and 4-chloro-2-(3,5-dimethyl-1*H*-pyrazol-1-yl)-6-methylpyrimidine (**1a**). Compound **1a** underwent a nucleophilic substitution reaction via its reaction with the corresponding 4-substituted cyclohexan-1-amine in anhydrous *N,N*-dimethylformamide (DMF) in the presence of *N,N*-diisopropylethylamine (DIPEA) at room temperature to afford **2a-f** in 77-84% yield.

The reaction of **1a** with 2-(4-nitrophenyl)ethan-1-amine and tyrosine analogues under a similar condition afforded compounds **2g-j** in 72-75% yield (Scheme 1).

Scheme 2 shows the synthesis of 4-aniline substituted analogs of 2-(3,5-dimethyl-1*H*-pyrazol-1-yl)-6-methylpyrimidine (**2k-v**) (47-83%) through the reaction of **1a** with different aniline derivatives in the presence of DIPEA and refluxing at 95 °C in DMF. Compound **2w** was also synthesized under the same conditions described for the synthesis of compounds **2k-v** by the reaction of **1a** and 5,6-dimethoxy-1*H*-benzimidazol-2-amine.

Furthermore, the impact of changing the position of the 3,5-dimethylpyrazole ring and replacing the methyl group with an amino group on the pyrimidine was investigated by replacing (**1a**) with 4-chloro-6-(3,5-dimethyl-1*H*-pyrazol-1-yl)pyrimidin-2-amine (**1b**) and its coupling with different halogen-substituted aniline derivatives affording compounds **3a-g**. In the same context, the 4-amino analog of 6-chloro-2-(3,5-dimethyl-1*H*-pyrazol-1-yl)pyrimidine-4-amine (**1c**) reacted with 3-chloro-4-fluoroaniline, yielding compound **4**. Likewise, compounds **5a-b**, **6a-b**, and **7** were synthesized as described in Scheme 3 from the reaction of appropriate anilino-substituted analogs of 4-chloro-6-methyl-2-(4-methyl-1*H*-imidazol-1-yl)pyrimidine (**1d**), 4-(4-chloro-6-methylpyrimidin-2-yl)-2-methyloxazole (**1e**), in which the pyrazole moiety was replaced by imidazolyl (**1d**) and oxazolyl (**1e**) moieties,

or replacing the pyrimidine ring with pyridazine ring as in 3-chloro-6-(3,5-dimethyl-1*H*-pyrazol-1-yl)-4-methylpyridazine (**1f**).

2.2. Structure-Activity Relationship

The activity of the compounds on potentiating rat $K_{Ca2.2a}$ channels is summarized in Tables 1–5. Most of the compounds fall into five different classes. In addition to modification of the cyclohexyl moiety of CyPPA, changing the position of the pyrazole attachment and replacing it with an oxazolyl or imidazolyl ring generated significantly different compounds from a previous NeuroSearch patent¹⁶. Some of these compounds, such as **5a** and **6b** with the imidazole and oxazole ring, respectively, showed comparable potency to CyPPA. Furthermore, compound **4**, having an amino group instead of the methyl group on the pyrimidine, exhibited a potency similar to CyPPA. We also modified the central backbone of the compound, replacing the pyrimidine ring with a pyridazine ring in compound **7** that displayed comparable potency to CyPPA. The most potent compounds **2o** and **2q** resulted from increasing the hydrophobicity by replacing the cyclohexyl moiety of CyPPA with a substituted phenyl moiety. Compounds **2o** and **2q** with a CLogP value of 4.74 are more hydrophobic than CyPPA (CLogP = 4.07). As such, we evaluated the correlation between a number of functional group modifications and potency, as a structure-activity relationship study complementary to the previous patent¹⁶.

2.2.1. Optimization of the cyclohexane/phenyl moiety—We first explored the impact of adding one substituent group at C4 of the cyclohexane moiety of CyPPA with OH (**2a**), NH₂ (**2b**), CH₂OH (**2c**), OCH₃ (**2d**), F (**2e**), and NO₂ (**2f**). The potency of the newly synthesized compounds compared to the template CyPPA was measured via inside-out patch clamp electrophysiology recordings with rat $K_{Ca2.2a}$ channels heterologously expressed in HEK293 cells (Figure 1A). Among these compounds, only compound **2d** with the methoxy group was able to potentiate the $K_{Ca2.2a}$ channel with a drastically larger EC₅₀ value of $49.72 \pm 11.3 \mu\text{M}$ (n = 9), compared with the EC₅₀ value of $7.48 \pm 1.58 \mu\text{M}$ for CyPPA (Figure 1B and Table 1). All other compounds were inactive on the $K_{Ca2.2a}$ channel. The responses induced by 10 μM Ca²⁺ are considered the maximal currents of the $K_{Ca2.x}$ channels¹¹. To evaluate the efficacy (E_{max}) of compounds on rat $K_{Ca2.2a}$ channels, the current amplitudes at –90 mV in response to a series of concentrations of compounds were normalized to that obtained at 10 μM Ca²⁺ (I / I_{max} (%), Figure 1C). Non-linear regression curve fitting yielded an E_{max} of $94.59 \pm 17.17 \%$ (n = 9) on rat $K_{Ca2.2a}$ channels for compound **2d**, which is comparable to the E_{max} of $85.60 \pm 11.22 \%$ (n = 8) of CyPPA (Figure 1D).

Recently, we identified the binding pocket for CyPPA between CaM C-lobe and the HA/HB helices in rat $K_{Ca2.2a}$ channels¹⁵. The binding interface between CaM and its substrates are largely hydrophobic. As such, we replaced the cyclohexane moiety with more hydrophobic monosubstituted and disubstituted phenyl groups and decorated it with one or more electron withdrawing groups, such as trifluoromethane, nitro, carboxylic or hydrogen sulfide groups. Compounds **2k** and **2l** with a thiol or nitro substitution on the phenyl ring, respectively, were inactive (Table 4). Compound **2v**, which has carboxylic acid and fluoro substituents, did

not seem to have achieved its maximal response on rat $K_{Ca2.2a}$ channels due to its limited solubility (Figure 2A). As such, we could not accurately calculate its EC_{50} and E_{max} values.

A single 4-trifluoromethane substituent (**2s**) did not significantly change the potency compared with CyPPA, with an EC_{50} value of $3.45 \pm 1.00 \mu M$ ($n = 6$) (Figures 2A and 2B). The potency of dihalogen substituted phenyl derivatives (**2n-r** and **2t**) was significantly increased compared with CyPPA (Figures 2A and 2B). Among them, compound (**2q**) potentiated rat $K_{Ca2.2a}$ channels with an EC_{50} value of $0.64 \pm 0.12 \mu M$ ($n = 6$), which is ~10-fold more potent than CyPPA. The EC_{50} value of (**2o**) is $0.99 \pm 0.19 \mu M$ ($n = 6$), which is ~7-fold more potent than CyPPA (Table 4). All of these compounds exhibited similar efficacy (E_{max}) on $K_{Ca2.2a}$ channels as CyPPA, except for **2v** (Figure 2C and Figure 2D). Thus, improvement of potency was achieved through halogen substitutions on the phenyl ring; dihalogen substitutions at the positions 2 and 5 or 3 and 4 of the phenyl ring especially induced ~10- and ~7-fold increases in potency, respectively.

Positive modulators potentiate the activity of $K_{Ca2.2a}$ channels through enhancing their apparent Ca^{2+} sensitivity¹¹. We tested the effects of compound **2o** and **2q** on the concentration-dependent activation of $K_{Ca2.2a}$ channels by Ca^{2+} (Figure 2E). In the presence of compound **2o** ($10 \mu M$) or **2q** ($10 \mu M$), $K_{Ca2.2a}$ channels were more sensitive to Ca^{2+} , with EC_{50} values to Ca^{2+} of $0.11 \pm 0.023 \mu M$ ($n = 7$) and $0.091 \pm 0.016 \mu M$ ($n = 6$), respectively, compared with an EC_{50} value to Ca^{2+} of $0.35 \pm 0.035 \mu M$ ($n = 5$) in the absence of positive modulators (Figure 2F).

2.2.2. Optimization of the linker between pyrimidine and phenyl—Compared with compounds **2a-f**, the cyclohexane was replaced with a substituted phenyl group and the amino linker between pyrimidine and phenyl moieties was extended by an ethylene in the structure of compound **2g**. Replacing a hydrogen atom in the ethylene linker of compound **2g** with an α -carboxylic group, together with replacing with different substituted phenyl group afforded compound **2h-j**. Compound **2g-j** lost activity on the rat $K_{Ca2.2a}$ channel (Tables 2 and 3).

2.2.3. Optimization of the pyrimidine moiety—Since **2o** achieved ~7-fold better potency than CyPPA, we used **2o** as a template for further optimization of the pyrimidine moiety. First, changing the position at which the dimethyl pyrazole moiety is attached from C2 to C6 and replacing the methyl group with an amino group as in compound **1b**, resulted in a loss of activity for compounds **3a-g** on the rat $K_{Ca2.2}$ channel (Table 5). Meanwhile, replacing the methyl group at C6 of the pyrimidine moiety with an amine afforded compound **4**. The replacement of pyrimidine ring with a pyridazine ring generated compound **7**. Both compounds **4** and **7** exhibited reduced potency with EC_{50} values of $6.59 \pm 1.55 \mu M$ and $4.32 \pm 0.85 \mu M$ (Figures 3A and 3B), compared to compound **2o**, respectively, while retaining their efficacy (Figures 3C and 3D).

2.2.4. Optimization of the pyrazole moiety—Compounds **2o** and **2q** were used as templates for further structure optimization of the pyrazole moiety. We investigated the effect of replacing the pyrazole moiety with other five membered heterocyclic ring systems to determine whether the pyrazole ring is required for the potentiation of rat

K_{Ca}2.2a channels by CyPPA. When the pyrazole ring was replaced by an imidazole ring, the resulting compounds were **5a** and **5b**. The replacement of the pyrazole ring with an oxazole afforded compounds **6a** and **6b**. Compounds **6a** exhibited lower potency than **2q** on potentiating rat K_{Ca}2.2a channels, whereas the potency of **5b** was drastically reduced compared with **2o** (Figures 4A and 4B). Compounds **5a**, **6a**, and **6b** retained their efficacy, while the E_{max} value of **5b** was decreased compared with **2o** (Figures 4C and 4D).

2.2.5. Channel subtype selectivity of the new compounds—As described above, 3-chloro-4-fluorophenyl and 5-chloro-2-fluorophenyl disubstituted 4-aniline substituted analogs of 2-(3,5-dimethyl-1*H*-pyrazol-1-yl)-6-methylpyrimidine (**2o** and **2q**) were the most potent CyPPA analogs. CyPPA selectively potentiates K_{Ca}2.2a and K_{Ca}2.3, but not K_{Ca}2.1 or K_{Ca}3.1 channel subtypes¹¹. We tested whether the two newly synthesized compounds, **2o** and **2q**, retained their subtype-selectivity. Neither **2o** (Figure 5A) nor **2q** (Figure 5B) elicited significant responses from the human K_{Ca}2.1 channel expressed in HEK293 cells. When compared with the responses from K_{Ca}2.2a channels to these two compounds, the differences became even more obvious (Figure 5C), with the E_{max} values on K_{Ca}2.2a channels at ~90%, whereas the E_{max} values on K_{Ca}2.1 channels were at ~0% (Figure 5D). Similarly, the human K_{Ca}3.1 channel expressed in HEK293 cells was mostly insensitive to the two newly synthesized compounds (Figure 6A). The E_{max} value of **2o** on K_{Ca}3.1 channels was 28.33 ± 17.87 % (n = 5), whereas the E_{max} values of **2q** on K_{Ca}3.1 channels was 2.02 ± 3.16 % (n = 10) (Figure 6B).

CyPPA has a slightly but significantly higher potency on K_{Ca}2.3 channels than K_{Ca}2.2a channels¹¹. We examined the effects of the two newly synthesized compounds on human K_{Ca}2.3 channels (Figure 7A). Compound **2o** potentiated human K_{Ca}2.3 channels with an EC₅₀ value of 0.19 ± 0.071 μM (n = 10), which was significantly smaller than its EC₅₀ value of 0.99 ± 0.19 μM (n = 6) on the rat K_{Ca}2.2 channel subtype. On the other hand, **2q** exhibited similar potency on the K_{Ca}2.2a and K_{Ca}2.3 channel subtypes, with EC₅₀ values of 0.64 ± 0.12 μM (n = 6) and 0.60 ± 0.10 μM (n = 9), respectively (Figure 7B). The E_{max} values of **2o** and **2q** were similar between the K_{Ca}2.2a and K_{Ca}2.3 channel subtypes (Figures 7C and 7D).

CyPPA inhibits the K_{Ca}1.1 and Na_v1.2 channels with IC₅₀ values in the micromolar range¹¹. In contrast, compounds **2o** and **2q** at 100 μM did not affect the human K_{Ca}1.1 channel current expressed in HEK293 cells (Figures 8A and 8B). Compounds **2o** and **2q** at 100 μM inhibited the Na_v1.2 sodium current by ~50% in N1E-115 neuroblastoma cells (expressing the mouse Na_v1.2 channel) (Figures 8C and 8D). Neither **2o** nor **2q** seem to have achieved the maximal response on Na_v1.2 channels even at 100 μM, in the partial concentration-response curves limited by solubility (Figures 8E). Collectively, these results suggest improved selectivity of compounds **2o** and **2q** for K_{Ca}2.2a/ K_{Ca}2.3 over other channels.

2.3. Normalization of cerebellar PC firing from SCA2-58Q transgenic mice by the new compounds

The accurate firing of cerebellar Purkinje cells (PCs) is crucial for proper cerebellar functioning. In our mouse model of SCA2, aging SCA2-58Q transgenic mice, we previously observed a gradually increasing portion of PCs with highly irregular bursting activity^{17, 18}. Consistent with our preceding results, in the current study we also observed that most PCs from 7-8 months old WT mice ($97 \pm 4\%$, $n = 56$ PCs) were firing tonically (examples of tonic patterns: Figures 9B *right* and 10B *right*), whereas far fewer PCs from SCA2 mice of the same age exhibited stable firing rates ($75 \pm 13\%$, $n = 119$ PCs, $**p < 0.01$). Thus, every fourth SCA2-58Q PCs exhibited bursting activity patterns (Figures 9B *left* and 10B *left*). We believe that highly irregular bursting activity reflects the consequences of the ionic imbalance observed in SCA2 PCs,¹⁹ leading to the motor decline in SCA2 mice^{17, 18, 20}. Thus, compounds that can convert bursting activity back into the tonic mode may have the potential therapeutic effects for SCA2 and other ataxias²¹.

To investigate if positive allosteric modulators of K_{Ca2} channels can rescue the abnormal firing of SCA2-58Q PCs, we performed a series of experiments with acute cerebellar slices from 7-8-month-old SCA2-58Q mice in the presence of the non-selective $K_{Ca2.x/K_{Ca3.1}}$ channel modulator CHZ (chlorzoxazone as a positive control) and the subtype-selective modulators **2o** and **2q**. Application of 50 μ M CHZ converted bursting SCA2-58Q PC to tonic firing pattern, and also significantly decreased the firing frequency of the cell and improved the regularity of PC activity (data not shown).

In our previously published study¹⁷, CyPPA was able to normalize activity of SCA2-58Q PCs in approximately 50% of experiments with cerebellar slices. In the present study, all the tested bursting PCs responded to the exposure to compounds **2o** and **2q** ($n = 8$ for **2o** and $n = 9$ for **2q**). Application of 10 μ M **2o** converted bursting SCA2-58Q PC to a tonic firing pattern in 7 out of 8 experiments (Figures 9A and 9B). In 1 out of 8 experiments the high-frequency bursts were converted into a low-frequency activity with gaps. Compound **2o** significantly decreased the firing frequency (Figure 9C). The average firing frequency before the exposure to compound **2o** was 182.8 ± 37.0 Hz, and 10 minutes after the exposure it was 74.4 ± 47.7 Hz ($n = 8$ PCs, $***p < 0.001$). Here we also analyzed the interspike interval (ISI) distribution before and after **2o** application, obtained from 10-s fragments of the recording (Figure 9C). The ISI distribution before the exposure to **2o** shows two peaks, whereas the ISI distribution after **2o** application trends to the normal distribution. The coefficient of variation (CV) of ISI before the exposure to compound **2o** was 1.30 ± 0.39 , and 10 minutes after the exposure it was 0.17 ± 0.26 ($n = 8$ PCs, $****p < 0.0001$).

Figure 10A shows a representative recording trace of a bursting PC before and after the exposure to compound **2q**. The fragments that were analyzed for firing frequency and CV ISI values are indicated by arrows in the bottom of Figure 10A. The representative 390-ms fragments of PC activity recordings before the exposure to **2q** and 7 min after the exposure are shown in Figure 10B. The firing frequency inside the bursts before the exposure to compound **2q** was 134.3 Hz, and the firing frequency after the exposure during the tonic mode was 55.9 Hz (Figure 10C). The CV of ISI before the exposure to compound **2q**

was 1.83, and 7 minutes after the exposure it was 0.21 (Figure 10C). The application of 10 μ M compound **2q** converted the bursting activity patterns into tonic mode in 9 out of 9 experiments. In 2 out of these 9 experiments, the PCs remained in tonic mode after **2q** application. In the other 7 experiments, the PCs were converted into tonic mode, before stopping firing completely within 15 ± 7 minutes after **2q** application (Figures 10A and 10B). It also significantly decreased the firing frequency and improved the regularity of firing (Figure 10C). The average firing frequency before the exposure to compound **2q** was 180.3 ± 30.4 Hz, and 7-10 minutes after the exposure but before the tonic mode went to the silent mode it was 62.7 ± 54.3 Hz ($n = 9$ PCs, **** $p < 0.0001$). Here we also analyzed the ISI distribution before and after **2q** application, obtained from 10-s fragments of the recording (Figure 10C). The ISI distribution before the exposure to **2q** shows a few peaks, whereas the ISI distribution after **2q** application trends to the normal distribution (Figure 10C). The CV of ISI before the exposure to compound **2q** was 1.24 ± 0.50 , and 7-10 minutes after the exposure but before the tonic mode went to the silent mode it was 0.17 ± 0.21 ($n = 9$ PCs, **** $p < 0.0001$). Overall, these results are consistent with the higher potency of **2q** compared to **2o**.

Interestingly, the application of compounds **2o** and **2q** had little effect on tonic SCA2-58Q PCs. The average firing frequency before the exposure to compound **2o** was 62.0 ± 28.7 Hz, and 10 minutes after the exposure it was 58.3 ± 25.3 Hz ($n = 7$ PCs, ns). The application of compound **2o** did not affect the CV of ISI of tonic PCs. The CV of ISI before the exposure to compound **2o** was 0.05 ± 0.01 , and 10 minutes after the exposure it was 0.05 ± 0.02 ($n = 7$ PCs, ns). The average firing frequency before the exposure to compound **2q** was 74.8 ± 39.8 Hz, and 10 minutes after the exposure it was 80.7 ± 50.4 Hz ($n = 7$ PCs, ns). The application of compound **2q** did not affect the CV of ISI of tonic PCs. The CV of ISI before the exposure to compound **2q** was 0.06 ± 0.03 , and 10 minutes after the exposure it was 0.06 ± 0.04 ($n = 7$ PCs, ns).

All together, these experiments suggested that activation of K_{Ca2} channels restored tonic firing of PCs in aging SCA2 mice and compound **2q** was somewhat more potent than compound **2o** in this assay. Based on these results, we concluded that application of positive allosteric modulators of K_{Ca2} channels results in a reliable increase in regularity of SCA2-58Q PC firing pattern and hereby may have potential therapeutic effects for SCA treatment.

3. CONCLUSIONS

The present study suggests that CyPPA is a viable template for subtype-selective positive modulation of $K_{Ca2.2a}/K_{Ca2.3}$ channels. Replacing the cyclohexane ring with more hydrophobic disubstituted phenyl groups improved the potency of the compounds on potentiating the $K_{Ca2.2a}$ channel, while retaining their subtype-selectivity. Newly developed compounds were able to normalize abnormal firing of PCs in cerebellar slices from SCA2 mouse model, suggesting the therapeutic potential of these compounds for treating symptoms of ataxia.

4. EXPERIMENTAL SECTION

4.1. Materials

Cis-4-aminocyclohexanol (97%, Chem Block), cis-4-nitrocyclohexan-1-amine hydrochloride salt (95%, Chem Space), *cis*-4-methoxy-cyclohexylamine (97%, J&W Pharmlab), *cis*-4-nitroaniline (95%, aa Blocks), *cis*-4-aminothiophenol (97%, Aldrich), *cis*-4-fluorocyclohexan-1-amine hydrochloride (>97%, Pharma Block Sciences), 4-aminocyclohexyl methanol (95%, Enamine), *cis*-1,4-diaminocyclohexane (>98%, aa block), (*L*)-2-amino-3-(4-cyanophenyl)propanoic acid, (*L*)-tyrosine, (*L*)-2-amino-3-(3,4-difluorophenyl)propanoic acid (97%, Sigma Aldrich), 4-chloro-2-fluoroaniline (99%, Acros organic), 3-chloro-4-fluoroaniline (95%), 2-chloro-5-fluoroaniline (95%), 5-chloro-2-fluoroaniline (95%), 4-trifluoromethyl)aniline, 3-chloro-4-trifluoromethyl)aniline (95%), 5-chloro-4-trifluoromethyl)aniline (95%), 3-chloroaniline (95%), 2,3-difluoroaniline, 2,5-difluoroaniline (95%) (aa block and Aldrich), 4-chloro-6-methyl-2-(2-methyl-1,3-oxazol-4-yl)pyrimidine (95%, Chem Space), 4-chloro-2-(3,5-dimethyl-1*H*-pyrazol-1-yl)-6-methylpyrimidine (95%, Chem Space), 3-chloro-6-hydrazinyl-4-methylpyridazine (95%, Ambeed), 4-chloro-6-(3,5-dimethyl)-1*H*-pyrazol-1-yl) (95%, Alalab), anhydrous *N,N*-dimethylformamide (DMF) (99.8%, Sigma-Aldrich), dichloromethane (DCM), ethyl acetate (Fischer Chemical), and acetonitrile HPLC grade (Fisher Chemical) were purchased from the respective commercial vendors. CyPPA was purchased from Alomone Labs, Jerusalem, Israel. CyPPA was dissolved in DMSO to make stock solution of 100 mM. The stock solution was then diluted in bath solution to the final concentrations for patch-clamp recordings. All prepared compounds were purified using flash chromatography followed by reverse phase HPLC purification using Gemini 10 mm C18 110A, LC column phenomenex, 250 × 21.2 mm, at flow rate 7 mL/min. All compounds were >95% pure by HPLC analysis.

The chemical structures of final products were characterized by nuclear magnetic resonance spectrometry (1D) measured on a Bruker NMR spectrometer (400 MHz). The chemical shifts were reported in parts per millions (ppm). The compounds' molecular weight was confirmed by a high-resolution mass spectroscopy time-of-flight electrospray mass spectrometer (Q-TOF, Compass Hystar 4.1, Bruker, USA).

4.2. Chemistry

General procedures for the synthesis of compounds 2a-j.—4-Chloro-2-(3,5-dimethyl-1*H*-pyrazol-1-yl)-6-methylpyrimidine (**1a**, 0.23 mmol, 51.0 mg) was dissolved in 2 mL of anhydrous *N,N*-dimethylformamide (DMF) and *N,N*-diisopropylethylamine (DIPEA) (3 mmol, 348 μ L) was added to the solution. Then, the proper amine (0.25 mmol, 1.09 Equiv.) was dissolved in a few mL of DMF and added dropwise over 20 min to the solution containing compound **1a**, with stirring at room temperature for 36-48 h. The progress of the reactions was monitored by TLC. After completion of the reactions, the solvent was evaporated under reduced pressure, and the crude products were purified by flash chromatography using dichloromethane (DCM), and ethyl acetate at gradient 2-50%.

(Cis)-4-((2-(3,5-Dimethyl-1*H*-pyrazol-1-yl)-6-methylpyrimidin-4-yl)amino)cyclohexan-1-ol (2a).—Compound **2a** was

prepared by the reaction of compound

1a with (cis)-4-aminocyclohexan-1-ol (0.25 mmol, 28.8 mg) as described in general procedure. Yield 82%, as white powder. ^1H NMR (400 MHz, DMSO- d_6) δ 1.11-1.37 and 1.77-1.96 (m, 8H, 4 CH_2 's of cyclohexane ring), 2.15 (s, 3H, 3- CH_3 of pyrazole ring), 2.20 (s, 3H, 6- CH_3 of the pyrimidine ring), 2.64-2.72 (m, 1H, CHNH of cyclohexane ring), 3.18 (s, 3H, 5- CH_3 of pyrazole ring), 3.64-3.83 (m, 1H, CHOH), 4.56 (d, $J = 4.4$ Hz, 1H, OH), 6.02 (s, 1H, H-4 of the pyrazole ring), 6.15 (s, 1H, H-5 of the pyrimidine ring), 7.38 (d, $J = 6.8$ Hz, 1H, NH). ^{13}C NMR (101 MHz, DMSO) δ 164.21, 162.69, 156.59, 148.00, 141.02, 108.66, 101.17 (aromatic carbons of the pyrimidine and pyrazole rings), 68.18, 48.55, 33.99, 30.23 (carbons for the cyclohexyl ring), 23.40, 14.40, 13.43 (three methyl (5- CH_3 and 3- CH_3 of pyrazole and 6- CH_3 of the pyrimidine ring)). HR-MS (ESI-qTOF) (m/z) [$\text{C}_{16}\text{H}_{23}\text{N}_5\text{O}$]: calcd 301.1903, found 302.76100 [$\text{M} + \text{H}$] $^+$, 324.5613 [$\text{M} + \text{Na}$] $^+$.

(Cis)- N^1 -(2-(3,5-Dimethyl-1H-pyrazol-1-yl)-6-methylpyrimidin-4-yl)cyclohexane-1,4-diamine (2b).—Compound **2b** was

prepared by reaction of compound **1a** (0.23 mmol, 51.0 mg) and (cis)-cyclohexane-1,4-diamine (0.25 mmol, 28.5 mg) Yield 64%, white powder. ^1H NMR (400 MHz, DMSO- d_6) δ : 1.36-1.45 (m, 4H of the cyclohexyl ring), 1.91-2.10 (m, 4H of the cyclohexyl ring), 2.26 (s, 3H, 3- CH_3 of pyrazole ring), 2.36 (s, 3H, 6- CH_3 of the pyrimidine ring), 2.60-2.72 (m, 2H, 1- H and H-4 of the cyclohexyl ring), 3.17 (s, 3H, 5- CH_3 of pyrazole ring), 3.72-3.91 (br, 2H, NH_2), 6.28 (s, 1H, H-4 of the pyrazole ring), 6.33 (s, 1H, H-5 of pyrimidine ring), 7.96-8.01 (br, 1H, NH). ^{13}C NMR (101 MHz, DMSO- d_6) δ : 167.586, 162.04, 158.01, 151.49, 143.03, 111.40, 101.27 (aromatic carbons of the pyrimidine and pyrazole rings), 49.21, 48.29, 29.39, 28.9 (carbons for the cyclohexyl ring), 20.41, 14.53, 13.42 (three methyl (5- CH_3 and 3- CH_3 of pyrazole and 6- CH_3 of the pyrimidine ring)). HR-MS (ESI-qTOF) (m/z) [$\text{C}_{16}\text{H}_{24}\text{N}_6$]: calcd 300.2062, found, 301.94 30 [$\text{M} + \text{H}$] $^+$, 323.7408 [$\text{M} + \text{Na}$] $^+$.

((Cis)-4-((2-(3,5-Dimethyl-1H-pyrazol-1-yl)-6-methylpyrimidin-4-yl)amino)cyclohexyl)methanol (2c).—Compound **2c** was prepared

by reaction of compound **1a** (0.23 mmol, 51.0 mg) and (cis)-4-aminocyclohexyl)methanol (0.25 mmol, 32.3 mg), as described in the general procedure. Yield 79%, white powder. ^1H NMR (400 MHz, DMSO- d_6) δ : 1.27-1.44 (m, 5H of cyclohexane ring), 1.71-1.83 (m, 4H of the cyclohexane ring), 2.15 (s, 3H, 3- CH_3 of pyrazole ring), 2.21 (s, 3H, 6- CH_3 of the pyrimidine ring), 2.60-2.73 (m, 1H, CHNH of cyclohexane ring), 3.06 (s, 3H, 5- CH_3 of pyrazole ring), 3.52 (d, 2H, $J = 6$ Hz, CH_2OH), 4.42 (t, 1H, $J = 5.2$, OH), 6.02 (s, 1H, H-4 of the pyrazole ring), 6.15 (s, 1H, H-5 of the pyrimidine ring), 7.41 (d, 1H, $J = 7.6$ Hz, NH). ^{13}C NMR (101 MHz, DMSO) δ 164.59, 160.47, 157.05, 148.44, 141.46, 109.07, 101.59 (aromatic carbons of the pyrimidine and pyrazole rings), 66.66, 49.88, 42.26, 32.39, 24.59 (CH_2OH and carbons for the cyclohexyl ring), 23.83, 14.85, 13.88 (three methyl (5- CH_3 and 3- CH_3 of pyrazole and 6- CH_3 of the pyrimidine ring)). HR-MS (ESI-qTOF) (m/z) [$\text{C}_{17}\text{H}_{25}\text{N}_5\text{O}$]: calcd 315.2059, found 316.6403 [$\text{M} + \text{H}$] $^+$.

2-(3,5-Dimethyl-1H-pyrazol-1-yl)- N -(cis)-4-methoxycyclohexyl)-6-methylpyrimidin-4-amine (2d).—Compound **2d** was prepared

by the reaction of compound **1a** (0.23 mmol, 51.0 mg) and

(cis)-4-methoxycyclohexan-1-amine (0.25 mmol, 32.3 mg). Yield (81%), white powder. ^1H NMR (400 MHz, DMSO- d_6) δ : 1.25-1.38, and 2.10-2.18 (m, 8H of the cyclohexane ring), 2.21 (s, 3H, 3- CH_3 of pyrazole ring), 2.29 (s, 1H, 6- CH_3 of the pyrimidine ring), 2.59-2.71 (m, 1H, CHNH), 3.02 (s, 3H, 5- CH_3 of pyrazole ring), 3.16-3.23 (m, 1H, CHOCH_3), 3.34 (s, 3H, OCH_3), 6.06 (s, 1H, H-4 of the pyrazole ring), 6.19 (s, 1H, H-5 of the pyrimidine ring) 7.40 (d, $J = 7.6$ Hz, 1H, NH). ^{13}C NMR (101 MHz, DMSO- d_6) δ : 162.62, 160.03, 156.60, 148.00, 141.01, 108.64, 101.15 (aromatic carbons of the pyrimidine and pyrazole rings), 80.02, 66.22, 54.90, 31.95, 28.21, 23.41, 14.41, 13.43 (OCH_3 , carbons for the cyclohexyl ring, three methyl (5- CH_3 and 3- CH_3 of pyrazole and 6- CH_3 of the pyrimidine ring)). HR-MS (ESI-qTOF) (m/z) [$\text{C}_{17}\text{H}_{25}\text{N}_5\text{O}$]: calcd 315.2059, found 316.3240 [$\text{M} + \text{H}$].

2-(3,5-Dimethyl-1H-pyrazol-1-yl)-N-(cis)-4-fluorocyclohexyl)-6-methylpyrimidin-4-amine (2e).—Compound **2e** was

prepared by the reaction of compound **1a** (0.23 mmol, 51.0 mg) and (cis)-4-fluorocyclohexan-1-amine (0.25 mmol, 29.3 mg). Yield (77%), white powder. ^1H NMR (400 MHz, DMSO- d_6) δ : 1.48-1.58 and 1.66-1.77, 1.92-2.01 (m, 8H of the cyclohexane ring), 2.19 (s, 3H, 3- CH_3 of pyrazole ring), 2.34 (s, 3H, 6- CH_3 of the pyrimidine ring), 2.61-2.71 (m, 1H, CHNH), 3.10 (s, 3H, 5- CH_3 of pyrazole ring), 3.16-3.17 (m, 1H, CH-F), 6.08 (s, 1H, H-4 of the pyrazole ring), 6.28 (s, 1H, H-5 of the pyrimidine ring), 7.55 (d, $J = 6.4$ Hz, 1H, NH). ^{13}C NMR (101 MHz, DMSO- d_6) δ 167.22, 160.07, 156.64, 148.04, 141.05, 108.67, 101.19 (aromatic carbons of the pyrazole and pyrimidine rings), 90.13 (d, C4-F, $^1J_{\text{CF}} = 176.1$ Hz), 54.67, (C-1 of the cyclohexyl ring), 32.12 (d, C-3 and C-5 of the cyclohexyl ring, $^2J_{\text{CF}} = 28.3$ Hz), 28.29 (d, C-2 and C-6 of the cyclohexyl ring, $^3J_{\text{CF}} = 7.0$ Hz), 23.45, 14.45, 13.47 (three methyl (5- CH_3 and 3- CH_3 of pyrazole and 6- CH_3 of the pyrimidine ring)). HR-MS (ESI-qTOF) (m/z) [$\text{C}_{16}\text{H}_{22}\text{FN}_5$]: calcd 303.1859, found 304.3240 [$\text{M} + \text{H}$] $^+$.

2-(3,5-Dimethyl-1H-pyrazol-1-yl)-6-methyl-N-(cis)-4-nitrocyclohexyl)pyrimidin-4-amine (2f).—Compound

2f was prepared by the reaction of compound **1a** (0.23 mmol, 51.0 mg) and (cis)-4-nitrocyclohexan-1-amine (0.25 mmol, 36.0 mg). Yield (77%), white powder. ^1H NMR (400 MHz, CD_3OD) δ : 1.37-1.47 and 1.95-2.05, 2.14-2.18 (m, 8H of the cyclohexane ring), 2.24 (s, 3H, 3- CH_3 of pyrazole ring), 2.56 (s, 3H, 6- CH_3 of the pyrimidine ring), 2.70-2.79 (m, 1H, CHNH), 3.17 (s, 3H, 5- CH_3 of pyrazole ring), 3.78-3.86 (m, 1H, CHNO_2 of cyclohexane ring), 5.95 (s, 1H, H-4 of the pyrazole ring), 6.56 (s, 1H, H-5 of the pyrimidine ring), 7.74 (d, $J = 6.0$ Hz, 1H, NH). ^{13}C NMR (101 MHz, DMSO) δ 170.35, 161.92, 155.91, 148.38, 141.06, 108.35, 99.89 (aromatic carbons of the pyrazole and pyrimidine rings), 87.85, 54.69, 29.65, 24.15, 23.79, 13.52, 13.30 (carbons of the cyclohexyl ring and three methyl (5- CH_3 and 3- CH_3 of pyrazole and 6- CH_3 of the pyrimidine ring)). HR-MS (ESI-qTOF) (m/z) [$\text{C}_{16}\text{H}_{22}\text{N}_6\text{O}_2$]: calcd, 330.1804, found 331.3850 [$\text{M} + \text{H}$] $^+$.

2-(3,5-Dimethyl-1H-pyrazol-1-yl)-6-methyl-N-(4-nitrophenethyl)pyrimidin-4-amine (2g).—Compound **2g** was prepared by the reaction of compound

1a (0.23 mmol, 51.0 mg) and 2-(4-nitrophenyl)ethan-1-amine (0.25 mmol, 41.5 mg). Yield (72%), yellowish powder. ^1H NMR (400 MHz, DMSO- d_6) δ : 2.16 (s, 3H, 3- CH_3 of pyrazole ring), 2.26 (s, 1H, 6- CH_3 of the

pyrimidine ring), 2.90 (t, $J = 7.2$ Hz, 2H, NHCH_2CH_2), 3.09 (s, 3H, 5- CH_3 of the pyrazole ring), 3.37 (t, 2H, $J = 7.2$ Hz, NHCH_2CH_2), 6.00 (s, 1H, H-4 of the pyrazole ring), 6.51 (s, 1H, H-5 of the pyrimidine ring), 7.46 (d, 2H, $J = 8.0$ Hz, $H-2$ and $H-6$ of the phenyl group), 7.60-7.71 (br. s, 1H, NH), 8.09 (d, 2H, $J = 8.00$ Hz $H-3$ and $H-5$ of the phenyl group). ^{13}C NMR (101 MHz, DMSO- d_6) δ ^{13}C NMR (101 MHz, DMSO- d_6) δ 167.62, 160.22, 156.65, 149.12, 145.90, 145.39, 141.07, 130.47, 124.81, 108.71, 101.22 (aromatic carbons of the pyrazole, pyrimidine and phenyl), 45.90, 34.05 (Ph- $\text{CH}_2\text{CH}_2\text{-NH}$), 24.52, 15.28, 13.49 (three methyl (5- CH_3 and 3- CH_3 of pyrazole and 6- CH_3 of the pyrimidine ring)). HR-MS (ESI-qTOF) (m/z) [$\text{C}_{18}\text{H}_{20}\text{N}_6\text{O}_2$]: calcd, 352.1648, found 353.3240 [M + H] $^+$.

(S)-3-(4-Cyanophenyl)-2-((2-(3,5-dimethyl-1H-pyrazol-1-yl)-6-methylpyrimidin-4-yl)amino)propanoic acid (2h).—Compound **2h** was prepared by

the reaction of compound **1a** (0.23 mmol, 51.0 mg) and (*L*)-2-amino-3-(4-cyanophenyl)propanoic acid (0.25 mmol, 47.5 mg). Yield (54%), yellowish powder. ^1H NMR (400 MHz, CDCl_3) δ : 2.32 (s, 3H, 3- CH_3 of pyrazole ring), 2.47 (s, 1H, 6- CH_3 of the pyrimidine ring), 3.11 (s, 3H, 5- CH_3 of the pyrazole ring), 3.17 (dd, $J = 4.4$ and 4.4 Hz, 1H, $\beta\text{-CH}_2$), 3.43 (dd, 1H, $J = 4.0$ and 5.2 Hz, $\beta\text{-CH}_2$), 3.91 (t, $J = 3.6$ Hz, 1H, $\alpha\text{-CH}$), 6.07 (s, 1H, H-4 of the pyrazole ring), 6.46 (s, 1H, H-5 of the pyrimidine ring), 7.06 (d, 2H, $J = 8.0$ Hz, $H-2$ and $H-6$ of the phenyl group), 7.43 (d, 2H, $J = 8.0$ Hz, $H-3$ and $H-5$ of the phenyl group), 7.70 (d, 1H, $J = 7.6$ Hz, NH), 11.19 (br. s, 1H, COOH). HR-MS (ESI-qTOF) (m/z) [$\text{C}_{20}\text{H}_{20}\text{N}_6\text{O}_2$]: calcd, 376.1648, found 377.1682 [M + H] $^+$.

((2-(3,5-Dimethyl-1H-pyrazol-1-yl)-6-methylpyrimidin-4-yl)-L-tyrosine (2i).—

Compound **2i** was prepared by the reaction of compound **1a** (0.23 mmol, 51.0 mg) and (*L*)-tyrosine (0.25 mmol, 49.3 mg, 1.09 Equiv.). Yield (54%), yellowish powder. ^1H NMR (400 MHz, DMSO) δ : 2.18 (s, 3H, 3- CH_3 of pyrazole ring), 2.34 (s, 1H, 6- CH_3 of the pyrimidine ring), 3.05 (s, 3H, 5- CH_3 of the pyrazole ring), 3.16 (dd, $J = 4.4$, 4.4 Hz, 1H, $\beta\text{-CH}_2$), 3.42 (dd, 1H, $J = 4.4$, 4.4 Hz, $\beta\text{-CH}_2$), 3.91 (t, $J = 7.6$ Hz, 1H, $\alpha\text{-CH}$), 6.09 (s, 1H, H-4 of the pyrazole ring), 6.50 (s, 1H, H-5 of the pyrimidine ring), 6.67 (d, 2H, $J = 7.2$ Hz, H-2, and H-6 of the phenyl group), 7.06 (d, 2H, $J = 7.2$ Hz, H-3, and H-5 of the phenyl group), 7.92 (d, 1H, $J = 7.6$ Hz, NH), 11.10 (br. s, 1H, COOH). HR-MS (ESI-qTOF) (m/z) [$\text{C}_{19}\text{H}_{21}\text{N}_5\text{O}_3$]: calcd 367.1644, found 368.1678 [M + H] $^+$.

(S)-3-(3,4-Difluorophenyl)-2-((2-(3,5-dimethyl-1H-pyrazol-1-yl)-6-methylpyrimidin-4-yl)amino)propanoic acid (2j).—Compound

2j was prepared by the reaction of compound **1a** (0.23 mmol, 51.0 mg) and (*L*)-2-amino-3-(3,4-difluorophenyl)propanoic acid (0.23 mmol, 49.9 mg). Yield (32%), white powder. ^1H NMR (400 MHz, CDCl_3) δ : 2.25 (s, 3H, 3- CH_3 of pyrazole ring), 2.44 (s, 1H, 6- CH_3 of the pyrimidine ring), 3.05 (s, 3H, 5- CH_3 of the pyrazole ring), 3.16 (dd, $J = 4.4$, 4.4 Hz, 1H, $\beta\text{-CH}_2$), 3.50 (dd, 1H, $J = 4.4$ and 4.4 Hz, $\beta\text{-CH}_2$), 3.93 (t, 1H, $J = 7.6$ Hz, $\alpha\text{-CH}$), 5.98 (s, 1H, H-4 of the pyrazole ring), 6.55 (s, 1H, H-5 of the pyrimidine ring), 7.00-7.08 (m, 2H, aromatic protons of phenyl group), 7.08 (dd, 1H, $J = 2.4$, 2.4 Hz, aromatic proton of phenyl group), 7.66 (dd, 1H, $J = 2.4$, 2.4 Hz, aromatic proton of phenyl group), 7.96 (br. s, 1H, NH). HR-MS (ESI-qTOF) (m/z) [$\text{C}_{19}\text{H}_{19}\text{F}_2\text{N}_5\text{O}_2$]: calcd 387.1507, found 388.1540 [M + H] $^+$.

General procedures for the synthesis of compounds 2k-w, 3a-3g, 4, 5a, 5b, 6a, 6b, and 7.—Compound **1a**, **1b**, **1c**, **1d**, or **1e** (0.23 mmol) was dissolved in 2 mL of anhydrous *N,N*-dimethylformamide (DMF), *N,N*-diisopropylethylamine (DIPEA) (3 mmol, 348 μ L) was added to the solution. Then, 0.25 mmol of the proper aniline or heterocyclic amine dissolved in 3 mL of DMF was added dropwise over 20 min. with stirring under reflux at 95 °C for 36-48 h. The progress of the reactions was monitored by TLC. After completion of the reactions, the solvent was evaporated under reduced pressure, and the crude products were purified by flash chromatography using DCM, and ethyl acetate at gradient 0-50%.

4-((2-(3,5-Dimethyl-1H-pyrazol-1-yl)-6-methylpyrimidin-4-yl)amino)-benzenethiol (2k).—Compound **2k** was prepared by

the reaction of compound **1a** (0.23 mmol, 51.0 mg) and 4-aminobenzenethiol (0.25 mmol, 31.3 mg). Yield (68%), yellow powder. ^1H NMR (400 MHz, DMSO- d_6): δ 2.17 (s, 3H, 3- CH_3 of pyrazole ring), 2.27 (s, 3H, 6- CH_3 of the pyrimidine ring), 2.31 (s, 3H, 5- CH_3 of the pyrazole ring), 5.23 (s, 1H, *SH*), 5.88 (s, 1H, H-4 of the pyrazole ring), 6.43 (s, 1H, H-5 of the pyrimidine ring), 6.66 (d, 2H, $J = 8.4$ Hz, H-2 & H-6 of the phenyl ring), 7.27 (d, 2H, $J = 8.8$ Hz, H-3 and H-5 of the phenyl ring). ^{13}C NMR (101 MHz, DMSO- d_6) δ 174.97, 167.60, 155.73, 151.06, 149.45, 142.00, 137.15, 114.92, 112.25, 109.54, 109.50 (aromatic carbons of the pyrazole and pyrimidine), 23.69, 14.26, 13.41 (three methyl (5- CH_3 and 3- CH_3 of pyrazole and 6- CH_3 of the pyrimidine ring)). HR-MS (ESI-qTOF) (m/z) [$\text{C}_{16}\text{H}_{17}\text{N}_5\text{S}$] calcd 311.1205, found 312.1303 [$\text{M} + \text{H}$] $^+$.

2-(3,5-Dimethyl-1H-pyrazol-1-yl)-6-methyl-N-(4-nitrophenyl)pyrimidin-4-amine (2l).—Compound **2l** was prepared by the reaction of compound **1a** (0.23 mmol, 51.0 mg) and 4-nitroaniline (0.25 mmol, 32.3 mg at 130 °C. Yield (66%), yellow powder). ^1H NMR (400 MHz, DMSO- d_6) δ : 2.23 (s, 3H, 3- CH_3 of pyrazole ring), 2.42 (s, 3H, 6- CH_3 of the pyrimidine ring), 2.56 (s, 3H, 5- CH_3 of the pyrazole ring), 6.13 (s, 1H, H-4 of the pyrazole ring), 6.70 (s, 1H, H-5 of the pyrimidine ring), 8.03 (d, 2H, $J = 9.2$ Hz, H-2 and H-6 of the phenyl ring), 8.23 (d, 2H, $J = 9.2$ Hz, H-3 and H-5 of the phenyl ring), 10.38-10.47 (br. s, 1H, *NH*). ^{13}C NMR (101 MHz, DMSO- d_6) δ 167.00, 160.66, 156.03, 149.11, 146.34, 141.57, 141.10, 125.08, 118.86, 109.28, 103.65 (aromatic carbons of the pyrazole and pyrimidine), 23.66, 14.45, 13.54 (three methyl (5- CH_3 and 3- CH_3 of pyrazole and 6- CH_3 of the pyrimidine ring)). HR-MS (ESI-qTOF) (m/z) [$\text{C}_{16}\text{H}_{16}\text{N}_7\text{O}_2$]: calcd 324.1335, found 348.3758 [$\text{M} + \text{Na}$] $^+$.

N-(2,3-Difluorophenyl)-2-(3,5-dimethyl-1H-pyrazol-1-yl)-6-methyl-pyrimidin-4-amine (2m).—Compound **2m** was prepared by the reaction of compound **1a** (0.23 mmol, 51.0 mg) and 2,3-difluoroaniline (0.25 mmol, 32.3 mg). Yield (47%), as

a white powder. ^1H NMR (400 MHz, CDCl_3) δ : 2.38 (s, 3H, 3- CH_3 of pyrazole ring), 2.47 (s, 3H, 6- CH_3 of the pyrimidine ring), 2.57 (s, 3H, 5- CH_3 of the pyrazole ring), 6.04 (s, 1H, H-4 of the pyrazole ring), 6.55 (s, 1H, H-5 of the pyrimidine ring), 7.00 (dd, 1H, $J = 8.0$ and 3.2 Hz, H-4 of the phenyl ring), 7.08 (dd, 1H, $J = 8.4$ and 3.2 Hz, H-6 of the phenyl ring), 7.41 (m, 1H, H-5 of the phenyl ring), 8.03 (s, 1H, *NH*). ^{13}C NMR (101 MHz, CDCl_3) 168.16, 162.65, 160.10, 154.47, 143.20 (aromatic carbons of the pyrazole and pyrimidine),

151.22 (dd, C-2 of the phenyl ring, $^1J_{CF} = 218.4$ Hz, $^2J_{CF} = 23.2$ Hz), 151.46 (dd, C-3 of the phenyl ring, $^1J_{CF} = 238.6$ Hz, $^3J_{CF} = 18.3$ Hz), 130.22 (dd, C-1 of the phenyl ring, $^2J_{CF} = 22.2$ Hz, $^3J_{CF} = 8.8$ Hz), 126.45 (d, C-5 of the phenyl ring, $^3J_{CF} = 8.8$ Hz), 118.50 (d, C-6 of the phenyl ring, $^3J_{CF} = 3.0$ Hz), 108.77 (dd, C-4 of the phenyl ring, $^2J_{CF} = 12.12$ Hz, $^3J_{CF} = 6.2$ Hz), 111.58, 101.56 (C-5 and C-3 the pyrazole and pyrimidine), 22.62, 15.12, 13.29 (three methyl (5- CH_3 and 3- CH_3 of pyrazole and 6- CH_3 of the pyrimidine ring). HR-MS (ESI-qTOF) (m/z) [$\text{C}_{16}\text{H}_{15}\text{F}_2\text{N}_5$]: calcd 315.1296, found 316.139984 [M + H]⁺.

***N*-(2,5-Difluorophenyl)-2-(3,5-dimethyl-1*H*-pyrazol-1-yl)-6-methylpyrimidin-4-amine (2n).**—Compound **2n** was prepared by reaction of compound **1a** (0.23

mmol, 51.0 mg) and 2,5-difluoroaniline (0.25 mmol, 32.3 mg). Yield (55%), white powder. ^1H NMR (400 MHz, CDCl_3) δ : 2.32 (s, 3H, 3- CH_3 of pyrazole ring), 2.47 (s, 3H, 6- CH_3 of the pyrimidine ring), 2.56 (s, 3H, 5- CH_3 of the pyrazole ring), 6.03 (s, 1H, H-4 of the pyrazole ring), 6.54 (s, 1H, H-5 of the pyrimidine ring), 6.84 (dt, 1H, $J = 8.0, 4.0$ Hz, H-4 of the phenyl ring), 7.09 (dt, 1H, $J = 9.6, 4.0$ Hz, H-3 of the phenyl ring), 7.52-7.62 (br. m, 1H, H-6 of the phenyl ring), 8.07-8.19 (br. s, 1H, NH). ^{13}C NMR (101 MHz, CDCl_3) δ 167.13, 160.73, 158.70 (C-4, C-6, C-2 aromatic carbons of pyrimidine), 158.73 (d, C-F, $^1J_{CF} = 237.4$ Hz), 149.69 (d, C-F, $^1J_{CF} = 238.26$ Hz), 149.91, 147.54 (C-3 and C-5 of aromatic carbons of the pyrazole), 129.06 (dd, C-1 of the phenyl ring, $^2J_{CF} = 23.2$ Hz, $^3J_{CF} = 11.1$ Hz), 128.07 (dd, C-3 of the phenyl ring, $^2J_{CF} = 24.2$, $^3J_{CF} = 12.1$ Hz), 115.76 (d, C-4 of the phenyl ring, $^2J_{CF} = 22.2$ Hz) 109.75 (dd, C-6 of the phenyl ring, $^2J_{CF} = 13.1$ Hz, $^3J_{CF} = 6.1$ Hz), 108.07, 98.15 (C-6 of the pyrazole ring, and C-5 of the pyrimidine ring), 23.91, 17.02, 14.27 (three methyl (5- CH_3 and 3- CH_3 of pyrazole and 6- CH_3 of the pyrimidine ring). HR-MS (ESI-qTOF) (m/z) [$\text{C}_{16}\text{H}_{15}\text{F}_2\text{N}_5$]: calcd 315.1296, found 316.4337 [M + H]⁺.

***N*-(3-Chloro-4-fluorophenyl)-2-(3,5-dimethyl-1*H*-pyrazol-1-yl)-6-methylpyrimidin-4-amine (2o).**—Compound **2o** was prepared by

the reaction of compound **1a** (0.23 mmol, 51.0 mg) and 3-chloro-4-fluoroaniline (0.25 mmol, 36.4 mg). Yield (83%), white powder. ^1H NMR (400 MHz, CDCl_3) δ 2.31 (s, 3H, 3- CH_3 of pyrazole ring), 2.39 (s, 3H, 6- CH_3 of the pyrimidine ring), 2.59 (s, 3H, 5- CH_3 of the pyrazole ring), 5.99 (s, 1H, H-4 of the pyrazole ring), 6.31 (s, 1H, H-5 of the pyrimidine ring), 7.14 (d, 1H, $J = 7.6$ Hz, H-6 of the phenyl ring), 7.15 (t, 1H, $J = 7.2$ Hz, H-5 of the phenyl ring), 7.24 (s, 1H, NH), 7.47 (dd, 1H, $J = 6.0, 2.4$ Hz, H-2 of the phenyl ring). ^{13}C NMR (101 MHz, CDCl_3) δ 168.01, 162.20, 156.99 (C-4, C-6, and C-2 of the pyrimidine ring), 155.66 (d, C-F, $^1J_{CF} = 248.5$ Hz), 151.03, 142.90 (C-5 and C-3 of the pyrazole), 134.79 (d, C-6 of the phenyl group, $^3J_{CF} = 3.0$ Hz), 125.60 (C-1 of the phenyl ring), 123.13 (d, C-2 of the phenyl group, $^3J_{CF} = 7.1$ Hz), 121.71 (d, C-3 of the phenyl group, $^2J_{CF} = 19.2$ Hz), 117.25 (d, C-5 of the phenyl ring, $^2J_{CF} = 22.2$ Hz), 110.09, 99.75 (C-4 of the pyrazole ring, and C-5 of the pyrimidine ring), 24.32, 15.45, 13.98 (three methyl (5- CH_3 and 3- CH_3 of pyrazole and 6- CH_3 of the pyrimidine ring). HR-MS (ESI-qTOF) (m/z) [$\text{C}_{16}\text{H}_{15}\text{ClFN}_5$]: calcd 331.1000, found 332.104126 [M + H]⁺.

***N*-(4-Chloro-2-fluorophenyl)-2-(3,5-dimethyl-1*H*-pyrazol-1-yl)-6-methylpyrimidin-4-amine (2p).**—Compound **2p** was prepared by the reaction

of compound **1a** (0.23 mmol, 51.0 mg) and 4-chloro-2-fluoroaniline (0.25 mmol, 36.4 mg).

Yield (79%), white powder. ^1H NMR (400 MHz, CDCl_3) δ : 2.23 (s, 3H, 3- CH_3 of pyrazole ring), 2.45 (s, 3H, 6- CH_3 of the pyrimidine ring), 2.47 (s, 3H, 5- CH_3 of the pyrazole ring), 6.03 (s, 1H, H-4 of the pyrazole ring), 6.68 (s, 1H, H-5 of the pyrimidine ring), 7.05 (t, 1H, $J = 8.8$ Hz, H-3 of the phenyl ring), 7.23 (td, 1H, $J = 6.0$ and 2.4 Hz, H-5 of the phenyl ring), 7.60 (dd, 1H, $J = 6.4$ and 2.4 Hz, H-6 of the phenyl ring), 10.14–10.57 (br, s, 1H, NH). ^{13}C NMR (101 MHz, CDCl_3) δ 161.98, 158.77 (C-4, and C-6 of the pyrimidine ring), 155.83 (d, C2-F, $^1J_{\text{CF}} = 249.5$ Hz), 153.45, 151.61, 143.95 (C-2 of the pyrimidine ring, C-5 and C-3 of the pyrazole ring), 133.74 (d, C-4 of the phenyl group, $^3J_{\text{CF}} = 3.0$ Hz), 125.35 (C-5 of the phenyl ring), 123.13 (d, C-6 of the phenyl group, $^3J_{\text{CF}} = 7.1$ Hz), 121.09 (C-1 of the phenyl group, $^2J_{\text{CF}} = 18.2$ Hz), 116.82 (C-3 of the phenyl ring, $^2J_{\text{CF}} = 22.2$ Hz), 112.39, 102.45 (C-4 of the pyrazole ring, and C-5 of the pyrimidine ring), 20.81, 15.23, 13.44 (three methyl (5- CH_3 and 3- CH_3 of pyrazole and 6- CH_3 of the pyrimidine ring)). HR-MS (ESI-qTOF) (m/z) [$\text{C}_{16}\text{H}_{15}\text{ClFN}_5$]: calcd 331.1000, found 332.108978 [M + H] $^+$.

***N*-(5-Chloro-2-fluorophenyl)-2-(3,5-dimethyl-1*H*-pyrazol-1-yl)-6-methylpyrimidin-4-amine (2q).**—Compound **2q** was

prepared by the reaction of compound **1a** (0.23 mmol, 51.0 mg) and 5-chloro-2-fluoroaniline (0.25 mmol, 36.4 mg). Yield (72%), white powder. ^1H NMR (400 MHz, CDCl_3) δ : 2.32 (s, 3H, 3- CH_3 of pyrazole ring), 2.48 (s, 3H, 6- CH_3 of the pyrimidine ring), 2.54 (s, 3H, 5- CH_3 of the pyrazole ring), 6.05 (s, 1H, H-4 of the pyrazole ring), 6.65 (s, 1H, H-5 of the pyrimidine ring), 7.10 (t, $J = 8.8$ Hz, 1H, H-3 of the phenyl ring), 7.13 (td, 1H, $J = 8.8$ and 2.4 Hz, 1H, H-4 of the phenyl ring), 7.73 (dd, 1H, $J = 6.8$ and 2.4 Hz, H-6 of the phenyl ring), 9.02–9.21 (br, s, 1H, NH). ^{13}C NMR (101 MHz, CDCl_3) δ 164.90, 161.81, 154.93 (C-4, C-6, and C-2 of the pyrimidine ring), 153.50 (d, C2-F, $^1J_{\text{CF}} = 207.1$ Hz), 151.94, 143.62 (C-5 and C-3 of the pyrazole ring), 129.54 (d, C-6 of the phenyl ring, $^3J_{\text{CF}} = 4.0$ Hz), 126.97 (d, C-1 of the phenyl ring, $^2J_{\text{CF}} = 21.2$ Hz), 125.94 (d, C-4 of the phenyl group, $^3J_{\text{CF}} = 8.1$ Hz), 124.69 (C-5 of the phenyl ring), 116.99 (d, C-3 of the phenyl ring, $^2J_{\text{CF}} = 21.2$ Hz), 111.07, 101.80 (C-4 of the pyrazole ring, and C-5 of the pyrimidine ring), 23.03, 15.13, 13.59 ((three methyl (5- CH_3 and 3- CH_3 of pyrazole and 6- CH_3 of the pyrimidine ring)). HR-MS (ESI-qTOF) (m/z) [$\text{C}_{16}\text{H}_{15}\text{ClFN}_5$]: calcd 331.1000, found 332.112122 [M + H] $^+$.

***N*-(2-Chloro-5-fluorophenyl)-2-(3,5-dimethyl-1*H*-pyrazol-1-yl)-6-methylpyrimidin-4-amine (2r).**—Compound **2r** was prepared

by the reaction of compound **1a** (0.23 mmol, 51.0 mg) and 2-chloro-5-fluoroaniline (0.25 mmol, 36.4 mg). Yield (79%), white powder. ^1H NMR (400 MHz, CDCl_3) δ : 2.29 (s, 3H, 3- CH_3 of pyrazole ring), 2.45 (s, 3H, 6- CH_3 of the pyrimidine ring), 2.54 (s, 3H, 5- CH_3 of the pyrazole ring), 6.00 (s, 1H, H-4 of the pyrazole ring), 6.50 (s, 1H, H-5 of the pyrimidine ring), 6.85 (td, 1H, $J = 8.0$, 2.8 Hz, H-6 of the phenyl ring), 7.40 (dd, 1H, $J = 8.8$ and 3.2 Hz, H-4 of the phenyl ring), 7.85 (dd, 1H, $J = 10.4$, and 2.8 Hz, H-3 of the phenyl ring), 8.01–8.09 (br, s, 1H, NH). ^{13}C NMR (101 MHz, CDCl_3) δ 170.50 (C-4 of the pyrimidine ring), 166.61 (C5-F, $^1J_{\text{CF}} = 245.4$ Hz), 165.421, 160.49, 155.57, 147.82 (C-6, C-2 of the pyrimidine ring, C-5 and C-3 of the pyrazole ring), 142.09 (d, C-6 of the phenyl ring, $^2J_{\text{CF}} = 12.1$ Hz), 135.79 (d, C-1 of the phenyl ring, $^3J_{\text{CF}} = 6.1$ Hz), 125.92 (C-2 of the phenyl ring), 117.17 (C-4 of the phenyl ring, $^2J_{\text{CF}} = 24.2$ Hz), 115.15 (C-3 of the phenyl ring, $^3J_{\text{CF}} = 8.1$ Hz), 107.75, 99.87 (C-4 of the pyrazole ring, and C-5 of the pyrimidine ring), 22.85, 15.20,

13.78 (three methyl (5- CH_3 and 3- CH_3 of pyrazole and 6- CH_3 of the pyrimidine ring)).
HR-MS (ESI-qTOF) (m/z) [$\text{C}_{16}\text{H}_{15}\text{ClFN}_5$]: calcd 331.1000, found 332.110931 [M + H]⁺.

2-(3,5-Dimethyl-1H-pyrazol-1-yl)-6-methyl-N-(4-(trifluoromethyl)-phenyl)pyrimidin-4-amine (2s).—Compound **2s** was

prepared by the reaction of compound **1a** (0.23 mmol, 51.0 mg) and 4-(trifluoromethyl)aniline (0.25 mmol, 40.3 mg). Yield (74%), white powder. ¹H NMR (400 MHz, CD_2Cl_2): δ 2.33 (s, 3H, 3- CH_3 of pyrazole ring), 2.47 (s, 3H, 6- CH_3 of the pyrimidine ring), 2.59 (s, 3H, 5- CH_3 of the pyrazole ring), 6.13 (s, 1H, H-4 of the pyrazole ring), 6.84 (s, 1H, H-5 of the pyrimidine ring), 7.56-7.65 (m, 4H, H-2, H-3, H-5, and H-6 of the phenyl ring), 10.18-10.50 (br. s, 1H, NH). ¹³C NMR (101 MHz, CD_2Cl_2): δ 164.68, 162.38, 156.55, 152.83, 144.84 (C-4, C-6, and C-2 of the pyrimidine ring, C-5 of the pyrazole ring, and C-3 of the pyrazole ring), 141.42 (C-NH of the phenyl group), 126.90 (d, C-3 and C-5 of the phenyl ring, ³J_{CF} = 3.0 Hz), 126.37 (d, C-4 of the phenyl ring, ²J_{CF} = 18.2 Hz), 123.64 (d, CF₃, ¹J_{CF} = 224.2 Hz), 122.65 (C-2 and C-6 of the phenyl ring), 112.08, 102.71 (C-4 of the pyrazole ring, and C-5 of the pyrimidine ring), 22.56, 15.58, and 13.46 (three methyl (5- CH_3 and 3- CH_3 of pyrazole and 6- CH_3 of the pyrimidine ring)).
HR-MS (ESI-qTOF) (m/z) [$\text{C}_{17}\text{H}_{16}\text{F}_3\text{N}_5$]: calcd 347.1358, found 348.3704 [M + H]⁺.

N-(3-Chloro-4-(trifluoromethyl)phenyl)-2-(3,5-dimethyl-1H-pyrazol-1-yl)-6-methyl-pyrimidin-4-amine (2t).—Compound **2t** was prepared by the

reaction of compound **1a** (0.23 mmol, 51.0 mg) and 3-chloro-4-(trifluoromethyl)aniline (0.25 mmol, 48.9 mg). Yield (77%), white powder. ¹H NMR (400 MHz, CD_2Cl_2) δ : 2.24 (s, 3H, 3- CH_3 of pyrazole ring), 2.40 (s, 3H, 6- CH_3 of the pyrimidine ring), 2.56 (s, 3H, 5- CH_3 of the pyrazole ring), 6.05 (s, 1H, H-4 of the pyrazole ring), 6.64 (s, 1H, H-5 of the pyrimidine ring), 7.44 (d, 1H, *J* = 8.4 Hz, H-6 of the phenyl ring), 7.55 (d, 1H, *J* = 8.4 Hz, H-2 of the phenyl ring), 7.84 (s, 1H, C5-*H* of the phenyl ring), 8.11-8.56 (br s, 1H, NH).
HR-MS (ESI-qTOF) (m/z) [$\text{C}_{17}\text{H}_{15}\text{ClF}_3\text{N}_5$]: calcd 381.0968, found 382.1094 [M + H]⁺.

N-(3-Chloro-5-(trifluoromethyl)phenyl)-2-(3,5-dimethyl-1H-pyrazol-1-yl)-6-methylpyrimidin-4-amine (2u).—Compound **2u** was prepared by the

reaction of compound **1a** (0.23 mmol, 51.0 mg) and 3-chloro-5-(trifluoromethyl)aniline (0.25 mmol, 48.9 mg). Yield (75%), white powder. ¹H NMR (400 MHz, CD_2Cl_2) δ : 2.25 (s, 3H, 3- CH_3 of pyrazole ring), 2.51 (s, 6H, 6- CH_3 of the pyrimidine ring and 5- CH_3 of the pyrazole ring), 6.10 (s, 1H, H-4 of the pyrazole ring), 6.80 (s, 1H, H-5 of the pyrimidine ring), 7.42 (s, 1H, H-2 of the phenyl ring), 7.69 (s, 1H, H-6 of the phenyl ring), 7.75 (s, 1H, H-4 of the phenyl ring), 10.00-10.39 (br. s, 1H, NH). ¹³C NMR (101 MHz, CD_2Cl_2) 162.58, 158.77, 154.58, 151.40, 144.89, (C-4, C-6, & C-2 of the pyrimidine ring C-5 and C-3 of the pyrazole ring), 139.48 (C-NH of the phenyl group), 135.79 (C-3 of the phenyl group), 132.89 (d, C-5 of the phenyl ring, ²J_{CF} = 33.3 Hz), 125.63 (CF₃, ¹J_{CF} = 134.33 Hz), 122.82 (d, C-4, ³J_{CF} = 3.0 Hz), 122.25 (C-2 of the phenyl ring), 118.13 (d, C-6, ³J_{CF} = 3.0), 113.28, 103.83 (C-6 of the pyrimidine ring and C-4 of the pyrazole ring), 20.84, 15.44, 13.52 (three methyl (5- CH_3 and 3- CH_3 of pyrazole and 6- CH_3 of the pyrimidine ring)).
HR-MS (ESI-qTOF) (m/z) [$\text{C}_{17}\text{H}_{15}\text{ClF}_3\text{N}_5$]: calcd 381.0968, found 382.106476 [M + H]⁺.

3-((2-(3,5-Dimethyl-1H-pyrazol-1-yl)-6-methylpyrimidin-4-yl)amino)-4-fluorobenzoic acid (2v).—Compound **2v** was prepared

by the reaction of compound **1a** (0.23 mmol, 51.0 mg) and 3-amino-4-fluorobenzoic acid (0.25 mmol, 38.8 mg). Yield (79%), white powder. ¹H NMR (400 MHz, CD₃OD) δ: 2.28 (s, 3H, 3-CH₃ of pyrazole ring), 2.32 (s, 3H, 6-CH₃ of the pyrimidine ring), 2.54 (s, 3H, 5-CH₃ of the pyrazole ring), 6.17 (s, 1H, H-4 of the pyrazole ring), 6.66 (s, 1H, H-5 of the pyrimidine ring), 7.38 (t, 1H, *J* = 8.8 Hz, H-5 of the phenyl ring), 8.0-8.04 (m, 1H, H-6 of the phenyl ring), 8.30 (dd, *J* = 2.0 and 2.0 Hz, H-2 of the phenyl ring). ¹³C NMR (101 MHz, CD₃OD) δ: 167.95, 164.66 (C-4 of the pyrimidine ring, COOH), 160.55 (d, C-4-F, ¹*J*_{C-F} = 256.54 Hz), 160.13 and 155.31 (C-6 and C-2 of the pyrimidine ring), 152.47, 145.91 (C-5 and C-3 of the pyrazole ring), 131.37 (d, C-2 of the phenyl ring, ³*J*_{CF} = 9.1 Hz), 130.33 (C-1 of the phenyl ring), 128.97 (d, C-6 of the phenyl ring, ³*J*_{CF} = 3.0 Hz), 125.98 (d, C-3 of the phenyl ring, ²*J*_{CF} = 13.1 Hz), 117.37 (d, C-5 of the phenyl ring, ²*J*_{CF} = 20.2 Hz), 113.46 and 102.97 (C-6 of the pyrimidine ring and C-4 of the pyrazole ring), 23.75, 15.07 and 13.60 (three methyl (5-CH₃ and 3-CH₃ of pyrazole and 6-CH₃ of the pyrimidine ring)). HR-MS (ESI-qTOF) (m/z) [[C₁₇H₁₆FN₅O₂]: calcd 341.1288, found 342.1322 [M + H]⁺.

N-(2-(3,5-Dimethyl-1H-pyrazol-1-yl)-6-methylpyrimidin-4-yl)-5,6-dimethoxy-1H-benzo[d]imidazol-2-amine (2w).—Compound **2w** was prepared by the reaction of

compound **1a** (0.23 mmol, 51.0 mg) and 5,6-dimethoxy-1H-benzo[d]imidazol-2-amine (0.25 mmol, 48.3 mg). Yield (75%), brown powder. ¹H NMR (400 MHz, CDCl₃) δ: 2.30 (s, 3H, 3-CH₃ of pyrazole ring), 2.39 (s, 3H, 6-CH₃ of the pyrimidine ring), 2.59 (s, 3H, 5-CH₃ of the pyrazole ring), 3.85 (s, 6H, 2 OCH₃), 5.95 (s, 1H, H-4 of the pyrazole ring), 6.52 (s, 1H, H-5 of the pyrimidine ring), 7.15 (d, 2H, H-2 and H-6 of the benzoimidazole ring), 7.85 (t, 2H, H-3 and H-4 of the benzoimidazole ring), 8.17 (s, 1H, NH), 11.24 (s, 1H, NH of the benzoimidazole ring). HR-MS (ESI-qTOF) (m/z) [C₁₉H₂₁N₇O₂]: calcd 379.1757, found 380.1990 [M + H]⁺.

N⁴-(3-Chlorophenyl)-6-(3,5-dimethyl-1H-pyrazol-1-yl)pyrimidine-2,4-diamine (3a).—Compound **3a** was prepared by the reaction of compound **1b** (4-chloro-6-(3,5-

dimethyl-1H-pyrazol-1-yl)pyrimidin-2-amine, 0.23 mmol, 51.2 mg) with 3-chloroaniline (0.25 mmol, 31.9 mg). Yield (45%), white powder. ¹H NMR (400 MHz, CD₃OD) δ 2.18 (s, 3H, 3-CH₃ of pyrazole ring), 2.50 (s, 3H, 5-CH₃ of pyrazole ring), 6.13 (s, 1H, H-5 of the pyrimidine ring), 6.33 (s, 1H, H-4 of the pyrazole ring), 7.08 (dd, 1H, *J* = 8.0 and 1.2 Hz, H-4 of phenyl ring), 7.26 (t, 1H, *J* = 8.0 Hz, H-5 of phenyl ring), 7.44 (dd, 1H, *J* = 8.0 and 1.2 Hz, H-6 of the phenyl ring), 7.74 (s, 1H, H-2 of the phenyl ring). ¹³C NMR (101 MHz, CD₃OD) δ 171.78, 161.83, 160.06, 153.81, 141.03 (C-4, C-6, and C-2 of the pyrimidine ring, C-5 and C-3 of the pyrazole ring), 135.77, 131.49, 124.92, 122.80, 121.01, 119.06 (6 carbons of the phenyl ring), 112.81, 85.89 (C-4 of the pyrazole ring and C-5 of the pyrimidine ring), 14.54, 13.58 (two methyl (5-CH₃ and 3-CH₃ of pyrazole)). HR-MS (ESI-qTOF) (m/z) [C₁₅H₁₅ClN₆]: calcd 314.1047, found 315.113220 [M + H]⁺.

N⁴-(3-Chloro-4-fluorophenyl)-6-(3,5-dimethyl-1H-pyrazol-1-yl)pyrimidine-2,4-diamine (3b).—Compound **3b** was prepared by the reaction of compound

1b (0.23 mmol, 51.2 mg) and 3-chloro-4-fluoroaniline (0.25 mmol, 36.4 mg).

Yield (65%) as a white powder. ^1H NMR (400 MHz, CD_3OD) δ 2.26 (s, 3H, 3- CH_3 of pyrazole ring), 2.57 (s, 3H, 5- CH_3 of pyrazole ring), 6.21 (s, 1H, H-5 of the pyrimidine ring), 6.38 (s, 1H, H-4 of the pyrazole ring), 7.24 (t, 1H, $J = 8.8$ Hz, H-5 of phenyl ring), 7.53 (dt, 1H, $J = 2.0, 4.0,$ and 9.2 Hz, H-6 of phenyl ring), 7.91 (dd, 1H, $J = 6.8, 2.8$ Hz, H-2 of phenyl ring). ^{13}C NMR (101 MHz, CD_3OD) δ 163.47, 159.07 (C-6, and C-4 of the pyrimidine ring), 156.39 (d, C4-F, $^1J_{\text{CF}} = 246.4$ Hz), 153.77, 152.41, 144.27 (C-2 of the pyrimidine ring, C-5 and C-3 of the pyrazole ring), 136.67 (d, C-6 of the phenyl group, $^3J_{\text{CF}} = 4.0$ Hz), 124.93 (C-NH of the phenyl ring), 123.07 (d, C-2 of the phenyl group, $^3J_{\text{CF}} = 7.1$ Hz), 122.07 (d, C-3 of the phenyl ring, $^2J_{\text{CF}} = 20.2$ Hz), 117.92 (d, C-5 of the phenyl ring, $^2J_{\text{CF}} = 22.2$ Hz), 112.75, 85.66 (C-4 of the pyrazole ring and C-5 of the pyrimidine ring), 14.47, 13.58 (two methyl (5- CH_3 and 3- CH_3 of pyrazole)). HR-MS (ESI-qTOF) (m/z) [$\text{C}_{15}\text{H}_{14}\text{ClFN}_6$]: calcd 332.0953, found 333.104126 [$\text{M} + \text{H}$] $^+$.

***N*⁴-(5-Chloro-2-fluorophenyl)-6-(3,5-dimethyl-1*H*-pyrazol-1-yl)pyrimidine-2,4-diamine (3c).**—Compound **3c** was prepared by the reaction of compound **1b** (0.23 mmol, 51.2 mg) and 5-chloro-2-fluoroaniline (0.25 mmol, 36.4 mg). Yield (72%) as a white powder. ^1H NMR (400 MHz, CD_3OD) δ 2.16 (s, 3H, 3- CH_3 of pyrazole ring), 2.58 (s, 3H, 5- CH_3 of pyrazole ring), 5.98 (s, 1H, H-5 of the pyrimidine ring), 6.48 (s, 1H, H-4 of the pyrazole ring), 6.85 (t, 1H, $J = 8.8$ Hz, H-3 of phenyl ring), 7.38 (td, 1H, $J = 8.4$ and 2.8 Hz, H-4 of phenyl ring), 7.84 (dd, $J = 6.4$ and 2.4 Hz, 1H, H-6 of phenyl ring). HR-MS (ESI-qTOF) (m/z) [$\text{C}_{15}\text{H}_{14}\text{ClFN}_6$]: calcd 332.0953 found 333.1150 [$\text{M} + \text{H}$] $^+$.

***N*⁴-(4-Chloro-2-fluorophenyl)-6-(3,5-dimethyl-1*H*-pyrazol-1-yl)pyrimidine-2,4-diamine (3d).**—Compound **3d** was prepared by the reaction of compound **1b** (0.23 mmol, 51.2 mg) and 4-chloro-2-fluoroaniline (0.25 mmol, 36.4 mg). Yield (54%) as a white powder. ^1H NMR (400 MHz, CD_3OD) δ 2.23 (s, 3H, 3- CH_3 of pyrazole ring), 2.57 (s, 3H, 5- CH_3 of pyrazole ring), 6.16 (s, 1H, H-5 of the pyrimidine ring), 6.47 (s, 1H, H-4 of the pyrazole ring), 7.22 (td, 1H, $J = 8.4, 2.4$ Hz, H-5 of phenyl ring), 7.29 (dd, 1H, $J = 10.8, 2.4$ Hz, H-6 of phenyl ring), 7.98 (t, 1H, $J = 8.8$ Hz, H-3 of phenyl ring). ^{13}C NMR (101 MHz, CD_3OD) δ 163.76, 159.32 (C-4 and C-6 of the pyrimidine ring), 158.52 (d, C2-F, $^1J_{\text{CF}} = 237.4$ Hz), 155.23, 153.70, 144.42 (C-2 of the pyrimidine ring, C-5 and C-3 of the pyrazole ring), 132.10 (d, C-4 of the phenyl group, $^3J_{\text{CF}} = 9.1$ Hz), 127.86 (C-5 of the phenyl ring), 126.14 (C-1 of the phenyl group, $^2J_{\text{CF}} = 11.1$ Hz), 125.91 (d, C-6 of the phenyl group, $^3J_{\text{CF}} = 4.0$ Hz), 117.60 (d, C-3 of the phenyl ring, $^2J_{\text{CF}} = 23.2$ Hz), 112.62, 85.38 (C-4 of the pyrazole ring and C-5 of the pyrimidine ring), 14.67, 13.39 (two methyl (5- CH_3 and 3- CH_3 of pyrazole)). HR-MS (ESI-qTOF) (m/z) [$\text{C}_{15}\text{H}_{14}\text{ClFN}_6$]: calcd 332.0952, found 334.1166 [$\text{M} + \text{H}$] $^+$.

***N*⁴-(2-Chloro-5-fluorophenyl)-6-(3,5-dimethyl-1*H*-pyrazol-1-yl)pyrimidine-2,4-diamine (3e).**—Compound **3e** was prepared by the reaction of compound **1b** (0.23 mmol, 51.2 mg) and 2-chloro-5-fluoroaniline (0.25 mmol, 36.4 mg). Yield (51%) as a white powder. ^1H NMR (400 MHz, CD_3OD) δ 2.15 (s, 3H, 3- CH_3 of pyrazole ring), 2.50 (s, 3H, 5- CH_3 of pyrazole ring), 6.03 (s, 1H, H-5 of the pyrimidine ring), 6.43 (s, 1H, H-4 of the pyrazole ring), 6.83 (td, 1H, $J = 9.2$ and 3.2 Hz, H-6 of phenyl ring), 7.37 (td, 1H, $J = 9.2$ and 3.2 Hz,

H-4 of phenyl ring), 7.82 (dd, 1H, $J = 10.4$ and 2.8 Hz, *H*-3 of phenyl ring). ^{13}C NMR (101 MHz, CD_3OD) δ 162.80 (d, C5-F, $^1J_{\text{CF}} = 245.4$ Hz), 163.00, 162.47, 152.97, 145.08, 144.15 (C-4, C-6, and C-2 of the pyrimidine ring, C-5 and C-3 of the pyrazole ring), 138.1 (d, C-6 of the phenyl group, $^2J_{\text{CF}} = 12.12$ Hz), 131.89 (d, C-1 of the phenyl group, $^3J_{\text{CF}} = 10.1$ Hz), 122.97 (C-2 of the phenyl group), 113.62 (d, C-4 of the phenyl group, $^2J_{\text{CF}} = 24.2$ Hz), 110.75 (C-3 of the phenyl group, $^3J_{\text{CF}} = 8.08$ Hz), 99.47, 86.23 (C-4 of the pyrazole ring and C-5 of the pyrimidine ring), 14.86, 13.59 (two methyl (5- CH_3 and 3- CH_3 of pyrazole)). HR-MS (ESI-qTOF) (m/z) [$\text{C}_{15}\text{H}_{14}\text{ClFN}_6$]: calcd 332.0953, found 334.1166 [$\text{M} + \text{H}$] $^+$.

***N*⁴-(2,5-Difluorophenyl)-6-(3,5-dimethyl-1*H*-pyrazol-1-yl)pyrimidine-2,4-diamine (3f).**—Compound **3f** was prepared by the reaction

of compound **1b** (0.23 mmol, 51.2 mg) and 2,5-difluoroaniline (0.25 mmol, 32.3 mg). Yield (53%) as a white powder. ^1H NMR (400 MHz, CD_3OD) δ 2.25 (s, 3H, 3- CH_3 of pyrazole ring), 2.58 (s, 3H, 5- CH_3 of pyrazole ring), 6.20 (s, 1H, *H*-5 of the pyrimidine ring), 6.57 (s, 1H, *H*-4 of the pyrazole ring), 6.88-6.94 (m, 1H, *H*-4 of phenyl ring), 7.17-7.23 (m, 1H, *H*-3 of phenyl ring), 8.03-8.08 (m, 1H, *H*-6 of phenyl ring). ^{13}C NMR (101 MHz, CD_3OD) δ 163.97, 159.60 159.02 (C-4, C-6, and C-2 of the pyrimidine ring), 159.94 (d, C-F, $^1J_{\text{CF}} = 241.4$ Hz), 153.72, 144.36 (C-5 and C-3 of the pyrazole ring), 153.26, 150.86 (d, C-F, $^1J_{\text{CF}} = 242.4$ Hz), 128.63 (d, C-1 of the phenyl ring, $^2J_{\text{CF}} = 22.2$ Hz, $^3J_{\text{CF}} = 9.0$ Hz), 117.25 (two d, C-3 and C-4 of the phenyl ring, $^2J_{\text{CF}} = 23.2$, 22.2 Hz, $^3J_{\text{CF}} = 9.1$ Hz), 112.55 (two d, C-6 of the phenyl ring, $^2J_{\text{CF}} = 23.2$ Hz, $^3J_{\text{CF}} = 8.1$ Hz), 112.47, 85.94 (C-4 of the pyrazole ring and C-6 of the pyrimidine ring), 14.61, 13.58 (two methyl (5- CH_3 and 3- CH_3 of pyrazole)). HR-MS (ESI-qTOF) (m/z) [$\text{C}_{15}\text{H}_{14}\text{F}_2\text{N}_6$]: calcd 316.1248, found, 318.1814 [$\text{M} + 2\text{H}$] $^+$.

***N*⁴-(3-Chloro-4-(trifluoromethyl)phenyl)-6-(3,5-dimethyl-1*H*-pyrazol-1-yl)pyrimidine-2,4-diamine (3g).**—Compound **3g** was prepared

by the reaction of compound **1b** (0.23 mmol, 51.2 mg) and 3-chloro-4-(trifluoromethyl)aniline (0.25 mmol, 48.9 mg). Yield (55%) as a white powder. ^1H NMR (400 MHz, CD_3OD) δ 2.25 (s, 3H, 3- CH_3 of pyrazole ring), 2.58 (s, 3H, 5- CH_3 of pyrazole ring), 6.16 (s, 1H, *H*-5 of the pyrimidine ring), 6.43 (s, 1H, *H*-4 of the pyrazole ring), 6.88 (d, 1H, $J = 8.8$ Hz, *H*-5 of phenyl ring), 7.76 (dd, 1H, $J = 8.8$, 1.2 Hz, *H*-6 of phenyl ring), 8.09 (s, 1H, *H*-2 of phenyl ring). ^{13}C NMR (101 MHz, CD_3OD) δ 163.93, 160.50, 154.24, 153.28 145.03, 144.11 (C-4, C-6, & C-2 of the pyrimidine ring, C-5 and C-3 of the pyrazole ring, C-NH of the phenyl ring), 133.54 (d, C-3 of the phenyl ring, $^3J_{\text{CF}} = 1.7$ Hz), 129.18 (C-5 of the phenyl ring, $^3J_{\text{CF}} = 5.0$ Hz), 128.60, 125.91 (C-6 of the phenyl ring and C-2 of the phenyl ring), 121.88 (d, CF_3 , $^1J_{\text{CF}} = 265.0$ Hz), 119.08 (d, C-4 of the phenyl ring, $^2J_{\text{CF}} = 12.0$ Hz), 112.22, 86.61 (C-4 of the pyrazole ring and C-6 of the pyrimidine ring), 14.50 and 13.48 (two methyl (5- CH_3 and 3- CH_3 of pyrazole)). HR-MS (ESI-qTOF) (m/z) [$\text{C}_{16}\text{H}_{14}\text{ClF}_3\text{N}_6$]: calcd 382.0921, found 384.113861 [$\text{M} + 2\text{H}$] $^+$.

***N*⁴-(3-Chloro-4-fluorophenyl)-2-(3,5-dimethyl-1*H*-pyrazol-1-yl)pyrimidine-4,6-diamine (4).**—Compound **4** was prepared by the reaction of compound **1c**

(4-chloro-(3,5-dimethyl-1*H*-pyrazol-1-yl)pyrimidine-6-amine, 0.23 mmol, 51.2 mg) and 3-chloro-4-fluoroaniline (0.25 mmol, 36.4 mg). Yield (73%), white powder. ^1H NMR (400 MHz, CD_3OD) δ 2.27 (s, 3H, 3- CH_3 of pyrazole ring),

2.55 (s, 3H, 5- CH_3 of pyrazole ring), 5.74 (s, 1H, H-5 of the pyrimidine ring), 6.17 (s, 1H, H-4 of the pyrazole ring), 7.23-7.31 (m, 2H, H-5 and H-6 of phenyl ring), 7.63 (dd, 1H, $J = 6.4, 2.4$ Hz, H-2 of the phenyl ring). ^{13}C NMR (101 MHz, CD_3OD) δ 163.05, 160.78 (C-4, and C-6 of the pyrimidine ring), 156.69 (d, C4-F, $^1J_{\text{CF}} = 247.4$ Hz), 153.88, 152.22, 145.31 (C-2 of the pyrimidine ring, C-5 and C-5 of the pyrazole ring), 136.74 (d, C-6 of the phenyl group, $^3J_{\text{CF}} = 3.0$ Hz), 126.64 (C-NH of the phenyl ring), 124.52 (d, C-2 of the phenyl group, $^3J_{\text{CF}} = 7.1$ Hz), 122.48 (C-3 of the phenyl group, $^2J_{\text{CF}} = 19.2$ Hz), 118.56 (C-5 of the phenyl ring, $^2J_{\text{CF}} = 22.2$ Hz), 112.59 (C-4 of the pyrazole ring), 80.89 (C-5 of the pyrimidine ring), 15.42 and 13.71 (two methyl (5- CH_3 and 3- CH_3 of pyrazole)). HR-MS (ESI-qTOF) (m/z) [$\text{C}_{15}\text{H}_{14}\text{ClFN}_6$]: calcd 332.0953, found 333.0991 [M + H] $^+$.

***N*-(5-Chloro-2-fluorophenyl)-6-methyl-2-(4-methyl-1*H*-imidazol-1-yl)pyrimidin-4-amine (5a).**—Compound **5a** was prepared by reaction of compound **1d** (4-chloro-6-methyl-2-(4-methyl-1*H*-imidazol-1-yl)pyrimidine, 0.24 mmol, 50.0 mg) and 5-chloro-2-fluoroaniline (0.25 mmol, 36.4 mg). Yield (71%), white powder. ^1H NMR (400 MHz, CD_3OD) δ : 2.37 (s, 3H, 4- CH_3 of imidazole ring), 2.43 (s, 3H, 6- CH_3 of the pyrimidine ring), 6.70 (s, 1H, H-5 of the pyrimidine ring), 7.19-7.25 (m, 2H, H-3 and H-4 of the phenyl ring), 7.84 (s, 1H, H-2 of imidazole ring), 7.95 (dd, 1H, $J = 6.8, 2.0$ Hz, H-6 of the phenyl ring), 9.25 (s, 1H, H-5 of the imidazole ring). ^{13}C NMR (101 MHz, CD_3OD) δ 169.38, 163.65 (C-4 and C-6 of the pyrimidine ring), 155.13 (d, C2-F, $^1J_{\text{CF}} = 244.4$ Hz), 153.57, 135.05, 133.99 (C-2 of the pyrimidine ring, C-2 and C-4 of the imidazole ring), 130.21 (d, C-6 of the phenyl group, $^3J_{\text{CF}} = 3.0$ Hz), 128.71 (d, C-1 of the phenyl ring, $^2J_{\text{CF}} = 13.1$ Hz), 126.58 (d, C-4 of the phenyl ring, $^3J_{\text{CF}} = 8.1$ Hz), 125.74 (C-5 of the phenyl ring), 118.12 (d, C-3 of the phenyl ring, $^2J_{\text{CF}} = 22.2$ Hz), 116.11, 105.76 (C-5 of the imidazole ring and C-5 of the pyrimidine ring), 23.74, 10.61 (two methyl (4- CH_3 of imidazole and 6- CH_3 of the pyrimidine ring)). HR-MS (ESI-qTOF) (m/z) [$\text{C}_{15}\text{H}_{13}\text{ClFN}_5\text{O}_3$]: calcd 317.0844, found 318.0922 [M + H] $^+$.

***N*-(3-Chloro-4-fluorophenyl)-6-methyl-2-(4-methyl-1*H*-imidazol-1-yl)pyrimidin-4-amine (5b).**—Compound **5b** was prepared by reaction of compound **1d** (0.24 mmol, 50.0 mg) and 3-chloro-4-fluoroaniline (0.25 mmol, 36.4 mg). Yield (76%), as white powder. ^1H NMR (400 MHz, CD_3OD) δ : 2.37 (s, 3H, 4- CH_3 of imidazole ring), 2.41 (s, 3H, 6- CH_3 of the pyrimidine ring), 6.59 (s, 1H, H-5 of the pyrimidine ring), 7.25 (t, 1H, $J = 8.8$ Hz, H-5 of the phenyl ring), 7.53-7.56 (m, 1H, H-6 of the phenyl ring), 7.72 (dd, 1H, $J = 6.8, 2.4$ Hz, H-2 of the phenyl ring), 7.90 (s, 1H, H-2 of imidazole ring), 9.29 (s, 1H, H-5 of the imidazole ring). ^{13}C NMR (101 MHz, CD_3OD) δ 168.78, 163.34 (d, C-4 and C-6 of the pyrimidine ring), 156.75 (d, C4-F, $^1J_{\text{CF}} = 245.4$ Hz), 153.65 (C-2 of the pyrimidine ring), 137.11 (d, C-6 of the phenyl group, $^3J_{\text{CF}} = 4.0$ Hz), 135.20 (C-2 and C-4 of the imidazole ring), 124.02 (C-NH of the phenyl ring), 122.31 (d, C-2 of the phenyl ring, $^3J_{\text{CF}} = 6.1$ Hz), 121.67 (d, C-3 of the phenyl ring, $^2J_{\text{CF}} = 19.2$ Hz), 117.88 (C-5 of the phenyl ring, $^2J_{\text{CF}} = 22.2$ Hz), 116.16 105.67 (C-5 of the imidazole ring C-5 of the pyrimidine ring), 23.69 and 10.68 (two methyl (4- CH_3 of imidazole and 6- CH_3 of the pyrimidine ring)). HR-MS (ESI-qTOF) (m/z) [$\text{C}_{15}\text{H}_{13}\text{ClFN}_5$]: calcd 317.0843; found, 318.0832.

***N*-(5-Chloro-2-fluorophenyl)-6-methyl-2-(2-methyloxazol-4-yl)pyrimidin-4-amine**

(6a).—Compound **6a** was prepared by reaction of compound **1e** (4-(4-chloro-6-methylpyrimidin-2-yl)-2-methyloxazole, 0.24 mmol, 50.3 mg) and 2-chloro-5-fluoroaniline (0.25 mmol, 36.4 mg),. Yield (74%), as a white powder. ¹H NMR (400 MHz, CD₃OD) δ 2.39 (s, 3H, 6-CH₃ of the pyrimidine ring), 2.50 (s, 3H, 2-CH₃ of oxazole ring), 6.60 (s, 1H, H-5 of the pyrimidine ring), 7.03-7.07 (m, 1H, H-4 of the phenyl ring), 7.13 (dd, 1H, *J* = 8.8, 2.0 Hz, H-3 of the phenyl ring), 8.24 (s, 1H, H-5 of the oxazole ring), 8.37 (dd, 1H, *J* = 6.8, 2.4 Hz, H-6 of the phenyl ring). ¹³C NMR (101 MHz, CD₃OD) δ 167.37, 164.10, 162.33 (C-4 and C-2 of the pyrimidine ring, and C-2 of the oxazole ring), 155.46 (d, C5-F, ¹*J*_{CF} = 245.4 Hz), 159.30, 141.53, 141.49 (C-6 of the pyrimidine ring, C-5 and C-4 of the oxazole ring), 130.15 (d, C-6 of the phenyl group, ³*J*_{CF} = 4.0 Hz), 129.95 (d, C-1 of the phenyl group, ²*J*_{CF} = 12.1 Hz), 124.49 (d, C-4 of the phenyl group, ³*J*_{CF} = 8.1 Hz), 124.27 (C-5 of the phenyl group), 117.44 (C-3 of the phenyl group, ²*J*_{CF} = 22.2 Hz), 105.25 (C-5 of the pyrimidine ring), 23.63, 13.66 (two methyl (2-CH₃ of oxazole and 6-CH₃ of the pyrimidine ring))HR-MS (ESI-qTOF) (m/z) [C₁₅H₁₂ClFN₄O]: calcd 318.06837, found 319.07254 [M + H]⁺.

***N*-(3-Chloro-4-fluorophenyl)-6-methyl-2-(2-methyloxazol-4-yl)pyrimidin-4-amine**

(6b).—Compound **6b** was prepared by reaction of compound **1e** (3-chloro-6-(3,5-dimethyl-1*H*-pyrazol-1-yl)-4-methylpyridazine, 0.24 mmol, 50.3 mg) and 3-chloro-4-fluoroaniline (0.25 mmol, 36.4 mg). Yield (81%), white powder. ¹H NMR (400 MHz, CD₃OD) δ 2.53 (s, 3H, 6-CH₃ of the pyrimidine ring), 2.57 (s, 3H, 2-CH₃ of oxazole ring), 6.68 (s, 1H, H-5 of the pyrimidine ring), 7.32 (t, 1H, *J* = 8.8 Hz, H-5 of the phenyl ring), 7.53-7.57 (m, 1H, H-6 of the phenyl ring), 7.79 (dd, 1H, *J* = 6.4, 2.4 Hz, H-2 of the phenyl ring), 8.61 (s, 1H, H-5 of the oxazole ring), 9.29 (s, 1 H, NH). ¹³C NMR (101 MHz, CD₃OD) δ 165.1 (d, C4-F, ¹*J*_{CF} = 207.1 Hz), 162.54, 158.78, 155.17 155.09, 145.20, 135.83 (C-4, C-2, C-6 of the pyrimidine ring, C-5 and C-4, and C-2 of the oxazole ring), 135.43 (d, C-6 of the phenyl group, ³*J*_{CF} = 3.0 Hz), 125.67 (C-NH of the phenyl ring), 123.92 (d, C-2 of the phenyl ring, ³*J*_{CF} = 5.1 Hz), 121.58 (C-3 of the phenyl ring, ²*J*_{CF} = 19.2 Hz), 118.19 (d, C-5 of the phenyl ring, ²*J*_{CF} = 23.2 Hz), 105.42 (C-5 of the pyrimidine ring), 19.51 and 13.60 (two methyl (2-CH₃ of oxazole and 6-CH₃ of the pyrimidine ring)). HR-MS (ESI-qTOF) (m/z) [C₁₅H₁₂ClFN₄O]: calcd 318.0683, found 319.0725 [M + H]⁺.

***N*-(3-Chloro-4-fluorophenyl)-6-(3,5-dimethyl-1*H*-pyrazol-1-yl)-4-methylpyridazin-3-amine (7).**

—Compound **7** was prepared by the reaction of compound **1f** (0.23 mmol, 51.2 mg) and 3-chloro-4-fluoroaniline (0.25 mmol, 36.4 mg). Yield (65%), white powder. ¹H NMR (400 MHz, CDCl₃) δ: 2.33 (s, 3H, CH₃ 3-CH₃ of pyrazole ring), 2.48 (s, 3H, 4-CH₃ of the pyridazine ring), 2.58 (s, 3H, 5-CH₃ of the pyrazole ring), 6.07 (s, 1H, H-4 of the pyrazole ring), 6.67 (s, 1H, H-5 of the pyridazine ring), 7.13 (t, 1H, *J* = 8.8 Hz, H-5 of the phenyl ring), 7.26-7.29 (m, 1H, H-6 of the phenyl ring), 7.60 (dd, 1H, *J* = 6.4, 2.0 Hz, H-2 of the phenyl ring), 9.84-10.10 (br s, 1H, NH). ¹³C NMR (101 MHz, CDCl₃) δ 161.99, 161.74 (C-3 and C-6 of the pyridazine ring), 153.55 (d, C4-F, ¹*J*_{CF} = 202.0 Hz), 157.02, 153.27, 143.75 (C-3 of the pyridazine ring, C-5 and C-3 of the pyrazole ring), 134.10 (d, C-6 of the phenyl group, ³*J*_{CF} = 3.0 Hz), 125.26 (C-NH of the phenyl ring), 123.13 (d, C-2 of the phenyl ring, ³*J*_{CF} = 7.1 Hz),

121.32 (d, C-3 of the phenyl ring, $^2J_{CF} = 19.2$ Hz), 117.03 (d, C-5 of the phenyl ring, $^2J_{CF} = 22.2$ Hz), 111.65, 101.72 (C-5 of the pyridazine ring and C-4 of the pyrazole ring), 22.16, 15.31, 13.58 (three methyl (5-CH₃ and 3-CH₃ of pyrazole and 4-CH₃ of the pyridazine ring). HR-MS (ESI-qTOF) (m/z) [C₁₆H₁₅ClFN₅]: calcd 331.1000, found 332.103271 [M + H]⁺.

4.3. Electrophysiology

The effect of newly synthesized compounds on K_{Ca}2.x/K_{Ca}3.1 channels was investigated as previously described^{14, 22}. Briefly, the rat K_{Ca}2.2a, human K_{Ca}2.1, human K_{Ca}2.3 or human K_{Ca}3.1 channel cDNA constructs were either generated in-house or through molecular cloning services (Genscript, Piscataway, NJ, USA). The channel cDNAs, along with CaM and GFP, at a ratio of 7:4:2 (ORF ratios), were transfected into HEK293 cells by the calcium-phosphate method. K_{Ca} currents were recorded 1–2 days after transfection, with an Axon200B amplifier (Molecular Devices, San Jose, CA, USA) at room temperature. The resistance of the patch electrodes ranged from 3–5 MΩ. The pipette solution contained (in mM): 140 KCl, 10 Hepes (pH 7.4), 1 MgSO₄. The bath solution containing (in mM): 140 KCl, 10 Hepes (pH 7.2), 1 EGTA, 0.1 Dibromo-BAPTA, and 1 HEDTA was mixed with Ca²⁺ to obtain the desired free Ca²⁺ concentrations, calculated using the software by Chris Patton of Stanford University (<https://somapp.ucdmc.ucdavis.edu/pharmacology/bers/maxchelator/webmaxc/webmaxcS.htm>). The Ca²⁺ concentrations were verified using a Ca²⁺ calibration buffer kit (Thermo Fisher Scientific). Briefly, a standard curve was generated using the Ca²⁺ buffers from the kit and a fluorescence Ca²⁺ indicator. Then, the Ca²⁺ concentrations of the bath solution were determined through interpolation on the standard curve.

High resistance seals (> 1 GΩ) were formed before inside-out patches were obtained. The seal resistance of inside-out patches was > 1 GΩ, when the intracellular face was initially exposed to a zero-Ca²⁺ bath solution. Currents were recorded by repetitive 1-s-voltage ramps from – 100 mV to + 100 mV from a holding potential of 0 mV. The currents were filtered at 2 kHz and digitized at a sampling frequency of 10 kHz. At the end of experiment, the integrity of the patch was examined by switching the bath solution back to the zero-Ca²⁺ buffer. Data from patches, which maintained the seal resistance (> 1 GΩ) after solution changes, were used for further analysis.

To measure the effect of CyPPA (Alomone Labs, Jerusalem, Israel) and newly synthesized compounds, the intracellular face was exposed to bath solutions with 0.15 μM Ca²⁺. One minute after switching of bath solutions, ten sweeps with a 1-s interval were recorded at a series of concentrations of compound in the presence of 0.15 μM Ca²⁺. The maximal K_{Ca}2.x/K_{Ca}3.1 current in response to 10 μM Ca²⁺ was then recorded.

For the K_{Ca}1.1 and Na_v1.2 channels, experiments were conducted using an EPC-10 amplifier (HEKA, Lambrecht/Pfalz, Germany). Cells were trypsinized and plated onto poly-L-lysine-coated coverslips. All recordings were done using normal Ringer solution as external bath solution. Patch pipettes were pulled from soda lime glass (micro-hematocrit tubes, Kimble Chase, Rochester, NY) and had resistances of 2–3 MΩ.

N1E-115 neuroblastoma cells (expressing mouse $\text{Na}_v1.2$ channels) were obtained from ATCC and cultured in complete DMEM. N1E-115 neuroblastoma cells were recorded with pipettes filled with internal solution consisted of (in mM) 10 NaF, 110 CsF, 20 CsCl, 10 HEPES, 2 EGTA, pH of 7.4 adjusted with CsOH, and osmolarity to 290-310 mOsm. Cells were pulsed for 200 msec at -120 mV from holding potential of -90 mV, then stepped up to either -10 mV or 0 mV for 50 msec to elicit inward currents, then back to -120 mV for 50 msec. Pulse interval was 0.1 Hz.

HEK-293 human $\text{K}_{\text{Ca}}1.1$ (BK) cells (gifted by Dr. Andrew Tinker, University College London) were recorded with internal pipette solution containing (in mM) 160 K^+ aspartate, 2.31 MgCl_2 , 10 HEPES, 10 EGTA, and 5.96 CaCl_2 (250 nM free Ca^{2+}), pH 7.2, 290–310 mOsm. Cells were held at -80 mV and pulsed by a step protocols from -80 mV to 80 mV, in 20 mV increments.

4.4. Data and statistical analysis

Patch-clamp recordings were analysed using Clampfit 10.5 (Molecular Devices LLC, San Jose, CA, USA) and concentration-response curves were analyzed in GraphPad Prism 9.0.2 (GraphPad Software Inc., La Jolla, CA, USA). To construct the concentration-dependent potentiation of channel activities by compound, the current amplitudes at -90 mV in response to various concentrations of the compound were normalized to that obtained at a maximal concentration of compound. The normalized currents were plotted as a function of the concentrations of the compound. EC_{50} values and Hill coefficients were determined by fitting the data points to a standard concentration–response curve ($Y = 100 / (1 + (X/\text{EC}_{50})^{\text{Hill}})$ – Hill). To assess the efficacy of compound, the current amplitudes obtained at the maximal concentration of the compound were normalized to the maximal $\text{K}_{\text{Ca}}2.x/\text{K}_{\text{Ca}}3.1$ current in response to $10 \mu\text{M}$ Ca^{2+} . Concentration-response curves were acquired from multiple patches for each data set. Each curve was fitted individually, which yielded the EC_{50} value for that curve. EC_{50} values are shown as mean \pm SD obtained from multiple patches, and the number of patches is indicated by n.

The Student's *t*-test was used for data comparison if there were only two groups. One-way ANOVA and Tukey's post hoc tests were used for data comparison of three or more groups. Post hoc tests were carried out only if F was significant and there was no variance in homogeneity.

4.5 Mice breeding and genotyping

Transgenic SCA2-58Q mice and their wild type (WT) littermates were used in these experiments. SCA2-58Q mice²³ were kindly provided to us by Dr. Stefan Pulst (University of Utah, Salt Lake City, Utah, USA) and were crossed to the FVB background strain. The breeding and genotyping of these mice were previously described^{20, 24, 25}. Briefly, hemizygous male SCA2-58Q mice were crossed with the WT female mice to generate mixed litters. The genotyping was done via PCR for *ATXN2* transgene as previously described^{20, 24, 25}. The volume of one PCR sample was 25 μl . The PCR mix per one sample contained: 2.5 μl 10 \times buffer for Taq polymerase, 0.5 μl 10 mM dNTP, 1.5 μl 25 mM MgCl_2 , 0.125 μl 20 μM primers (forward and reverse), 0.25 μl Taq

polymerase, 2 μ l DNA, and 18 μ l dH₂O. The sequence of the forward primer is: 5'-GCGAACACAAAGAGAAGGACCTGGA-3'. The sequence of the reverse primer is: 5'-GCCCTTGCTTCCCGTTTTAA-3'. The PCR product has 232 bp. Mice were housed in groups of two to six in one cage in the vivarium. The temperature was kept 22-24 °C including 12 daylight hours. The animals had access to standard food and water *ad libitum*. All procedures were approved by the Bioethics Committee of the Peter the Great St. Petersburg Polytechnic University at St. Petersburg, Russia, and followed the principles of the European convention (Strasbourg, 1986) and the Declaration of International medical association about humane treatment of animals (Helsinki, 1996).

4.6 Cerebellar slice recordings of spontaneous PC activity in SCA2-58Q mice

Recordings of spontaneous PC activity from WT and SCA2-58Q mice at 7-8 months of age were performed as previously described^{17, 18, 26}. Briefly, the mice were anesthetized with 2,000 mg/kg urethane and transcardially perfused with ice-cold aCSF containing (mM) 85 NaCl, 24 NaHCO₃, 25 glucose, 2.5 KCl, 0.5 CaCl₂, 4 MgCl₂, 1 NaH₂PO₄, 75 sucrose. Solutions were equilibrated with carbogen (95% O₂/5% CO₂). Next, the cerebellum was dissected and 300 μ m thick sagittal slices were cut with a VT1200S vibratome (Leica). Slices were recovering in aCSF containing (in mM) 119 NaCl, 26 NaHCO₃, 11 glucose, 2.5 KCl, 2.5 CaCl₂, 1.3 MgCl₂, 1 NaH₂PO₄ at 35 °C for 30-40 min and then transferred to the room temperature before recordings started. The external bath solution used for the recording was the same as the recovery aCSF, but also contained 100 μ M picrotoxin (PTX) and 10 μ M 6,7-dinitroquinoxaline-2,3-dione (DNQX), equilibrated with carbogen. All recordings were made within 5-6 hours after cerebellum was dissected. The recording chamber was heated to 35 °C using TC-324C automatic temperature controller (Warner Instruments, Hamden, CT). Loose-patch recordings were made as described previously^{17, 18} to evaluate the spontaneous activity of cerebellar PCs. Briefly, 1-3 M Ω glass pipettes were filled with the internal solution containing 140 mM NaCl buffered with 10 mM HEPES pH 7.3 and held at 0 mV. A loose patch (<100 M Ω) configuration was established at the PC soma at the axon hillock area. Spontaneous action potential currents were recorded for 5-60 min from each cell using Axon Multiclamp 700B amplifier (Molecular Devices, Sunnyvale, CA). The 10 min recordings were analyzed for tonic or burst firing as we previously described^{17, 18, 20}. Cells were characterized as firing tonically if they fired repetitive nonhalting spike trains for 10 min. A cell was characterized as bursting if it had more than 5% of the interspike intervals that fell outside of 3 SD from the mean of all interspike intervals in that cell. The analysis of PC firing was performed using Clampfit 10.2 (Molecular Devices). Data was plotted as the instantaneous firing rate every 100 ms for the entire recording duration. Once a bursting activity was established during the first 15-20 min of recordings, the bath solution was switched to the aCSF containing 50 μ M CHZ, 10 μ M **2o** or 10 μ M **2q** for at least 20 min to determine the effect of the compound on the firing pattern of that PC.

Supplementary Material

Refer to Web version on PubMed Central for supplementary material.

ACKNOWLEDGEMENTS

We are grateful to Lucia Basilio, Young Hur and Misa Nguyen for technical assistance. The authors also acknowledge the support of the core facility at Chapman University School of Pharmacy.

Funding Sources

M.Z. was supported by a YI-SCA grant from National Ataxia Foundation. IB holds the Carl J. and Hortense M. Thomsen Chair in Alzheimer's Disease Research. This work was supported by the National Institutes of Health grants 4R33NS101182 (I.B. and M.Z.) and R01NS056224 (I.B.) as well as by the strategic academic leadership program 'Priority 2030' of the Russian Federation (Agreement 75-15-2021-1333 30.09.2021 to SPbPU).

ABBREVIATIONS

CaM	calmodulin
CyPPA	<i>N</i> -cyclohexyl-2-(3,5-dimethyl-1 <i>H</i> -pyrazol-1-yl)-6-methylpyrimidin-4-amine
DCM	dichloromethane
DIPEA	<i>N,N</i> -diisopropylethylamine
DMF	<i>N,N</i> -dimethylformamide
K_{Ca}2.1 channels	small-conductance Ca ²⁺ -activated potassium subtype 1 channels
K_{Ca}2.2 channels	small-conductance Ca ²⁺ -activated potassium subtype 2 channels
K_{Ca}2.3 channels	small-conductance Ca ²⁺ -activated potassium subtype 3 channels
K_{Ca}3.1 channels	intermediate-conductance Ca ²⁺ -activated potassium channels
PCs	Purkinje cells
SCA	spinocerebellar ataxia

REFERENCES

1. Womack MD; Khodakhah K, Somatic and dendritic small-conductance calcium-activated potassium channels regulate the output of cerebellar Purkinje neurons. *J. Neurosci* 2003, 23 (7), 2600–2607. [PubMed: 12684445]
2. Geschwind DH; Perlman S; Figueroa CP; Treiman LJ; Pulst SM, The prevalence and wide clinical spectrum of the spinocerebellar ataxia type 2 trinucleotide repeat in patients with autosomal dominant cerebellar ataxia. *Am J Hum Genet* 1997, 60 (4), 842–850. [PubMed: 9106530]
3. Lastres-Becker I; Rub U; Auburger G, Spinocerebellar ataxia 2 (SCA2). *Cerebellum* 2008, 7 (2), 115–124. [PubMed: 18418684]
4. Brown BM; Shim H; Christophersen P; Wulff H, Pharmacology of small- and intermediate-conductance calcium-activated potassium channels. *Annu Rev Pharmacol Toxicol* 2020, 60, 219–240. [PubMed: 31337271]

5. Hosy E; Piochon C; Teuling E; Rinaldo L; Hansel C, SK2 channel expression and function in cerebellar Purkinje cells. *J Physiol* 2011, 589 (Pt 14), 3433–3440. [PubMed: 21521760]
6. Cingolani LA; Gymnopoulos M; Boccaccio A; Stocker M; Pedarzani P, Developmental regulation of small-conductance Ca^{2+} -activated K^{+} channel expression and function in rat Purkinje neurons. *J Neurosci* 2002, 22 (11), 4456–4467. [PubMed: 12040053]
7. Sailer CA; Kaufmann WA; Marksteiner J; Knaus HG, Comparative immunohistochemical distribution of three small-conductance Ca^{2+} -activated potassium channel subunits, SK1, SK2, and SK3 in mouse brain. *Mol Cell Neurosci* 2004, 26 (3), 458–469. [PubMed: 15234350]
8. Kuramoto T; Yokoe M; Kunisawa N; Ohashi K; Miyake T; Higuchi Y; Yoshimi K; Mashimo T; Tanaka M; Kuwamura M; Kaneko S; Shimizu S; Serikawa T; Ohno Y, Tremor dominant Kyoto (Trdk) rats carry a missense mutation in the gene encoding the SK2 subunit of small-conductance Ca^{2+} -activated K^{+} channel. *Brain research* 2017, 1676, 38–45. [PubMed: 28917524]
9. Balint B; Guerreiro R; Carmona S; Dehghani N; Latorre A; Cordvari C; Bhatia KP; Bras J, *KCNN2* mutation in autosomal-dominant tremulous myoclonus-dystonia. *Eur J Neurol* 2020, 27 (8), 1471–1477. [PubMed: 32212350]
10. Mochel F; Rastetter A; Ceulemans B; Platzer K; Yang S; Shinde DN; Helbig KL; Lopergolo D; Mari F; Renieri A; Benetti E; Canitano R; Waisfisz Q; Plomp AS; Huisman SA; Wilson GN; Cathey SS; Louie RJ; Del Gaudio D; Waggoner D; Kacker S; Nugent KM; Roeder ER; Bruel AL; Thevenon J; Ehmke N; Horn D; Holtgrewe M; Kaiser FJ; Kamphausen SB; Abou Jamra R; Weckhuysen S; Dalle C; Depienne C, Variants in the SK2 channel gene (*KCNN2*) lead to dominant neurodevelopmental movement disorders. *Brain* 2020, 143 (12), 3564–3573. [PubMed: 33242881]
11. Hougaard C; Eriksen BL; Jorgensen S; Johansen TH; Dyhring T; Madsen LS; Strobaek D; Christophersen P, Selective positive modulation of the SK3 and SK2 subtypes of small conductance Ca^{2+} -activated K^{+} channels. *British journal of pharmacology* 2007, 151 (5), 655–665. [PubMed: 17486140]
12. Lee CH; MacKinnon R, Activation mechanism of a human SK-calmodulin channel complex elucidated by cryo-EM structures. *Science* 2018, 360 (6388), 508–513. [PubMed: 29724949]
13. Cho LT; Alexandrou AJ; Torella R; Knafels J; Hobbs J; Taylor T; Loucif A; Konopacka A; Bell S; Stevens EB; Pandit J; Horst R; Withka JM; Pryde DC; Liu S; Young GT, An intracellular allosteric modulator binding pocket in SK2 ion channels is shared by multiple chemotypes. *Structure* 2018, 26 (4), 533–544 e3. [PubMed: 29576321]
14. Nam YW; Cui M; Orfali R; Viegas A; Nguyen M; Mohammed EHM; Zoghebi KA; Rahighi S; Parang K; Zhang M, Hydrophobic interactions between the HA helix and S4-S5 linker modulate apparent Ca^{2+} sensitivity of SK2 channels. *Acta Physiol (Oxf)* 2021, 231 (1), e13552. [PubMed: 32865319]
15. Nam YW; Cui M; El-Sayed NS; Orfali R; Nguyen M; Yang G; Rahman MA; Lee J; Zhang M, Subtype-selective positive modulation of $\text{K}_{\text{Ca}2}$ channels depends on the HA/HB helices. *British journal of pharmacology* 2021, 1–13.
16. Eriksen BL; Teuber L; Hougaard C; Sørensen US, Pyrazolyl-pyrimidines as potassium channel modulating agents and their medical use. W.O. Patent 2006/100212 A1. September 28, 2006.
17. Kasumu AW; Hougaard C; Rode F; Jacobsen TA; Sabatier JM; Eriksen BL; Strobaek D; Liang X; Egorova P; Vorontsova D; Christophersen P; Ronn LC; Bezprozvanny I, Selective positive modulator of calcium-activated potassium channels exerts beneficial effects in a mouse model of spinocerebellar ataxia type 2. *Chem Biol* 2012, 19 (10), 1340–1353. [PubMed: 23102227]
18. Kasumu AW; Liang X; Egorova P; Vorontsova D; Bezprozvanny I, Chronic suppression of inositol 1,4,5-triphosphate receptor-mediated calcium signaling in cerebellar purkinje cells alleviates pathological phenotype in spinocerebellar ataxia 2 mice. *J Neurosci* 2012, 32 (37), 12786–12796. [PubMed: 22973002]
19. Egorova PA; Bezprozvanny IB, Molecular mechanisms and therapeutics for spinocerebellar ataxia type 2. *Neurotherapeutics : the journal of the American Society for Experimental NeuroTherapeutics* 2019, 16 (4), 1050–1073. [PubMed: 31435879]
20. Egorova PA; Zakharova OA; Vlasova OL; Bezprozvanny IB, In vivo analysis of cerebellar Purkinje cell activity in SCA2 transgenic mouse model. *J Neurophysiol* 2016, 115 (6), 2840–2851. [PubMed: 26984424]

21. Egorova PA; Bezprozvanny IB, Electrophysiological studies support utility of positive modulators of SK channels for treatment of spinocerebellar ataxia type 2. *Cerebellum* 2021, In press.
22. Nam YW; Baskoylu SN; Gazgalis D; Orfali R; Cui M; Hart AC; Zhang M, A V-to-F substitution in SK2 channels causes Ca²⁺ hypersensitivity and improves locomotion in a *C. elegans* ALS model. *Scientific reports* 2018, 8 (1), 10749. [PubMed: 30013223]
23. Huynh DP; Figueroa K; Hoang N; Pulst SM, Nuclear localization or inclusion body formation of ataxin-2 are not necessary for SCA2 pathogenesis in mouse or human. *Nat Genet* 2000, 26 (1), 44–50. [PubMed: 10973246]
24. Egorova PA; Gavrilova AV; Bezprozvanny IB, In vivo analysis of the climbing fiber-Purkinje cell circuit in SCA2-58Q transgenic mouse model. *Cerebellum* 2018, 17 (5), 590–600. [PubMed: 29876801]
25. Egorova PA; Gavrilova AV; Bezprozvanny IB, In vivo analysis of the spontaneous firing of cerebellar Purkinje cells in awake transgenic mice that model spinocerebellar ataxia type 2. *Cell Calcium* 2021, 93, 102319. [PubMed: 33248384]
26. Egorova PA; Gavrilova AV; Bezprozvanny IB, Ataxic symptoms in Huntington's disease transgenic mouse model are alleviated by chlorzoxazone. *Front Neurosci* 2020, 14, 279. [PubMed: 32317916]

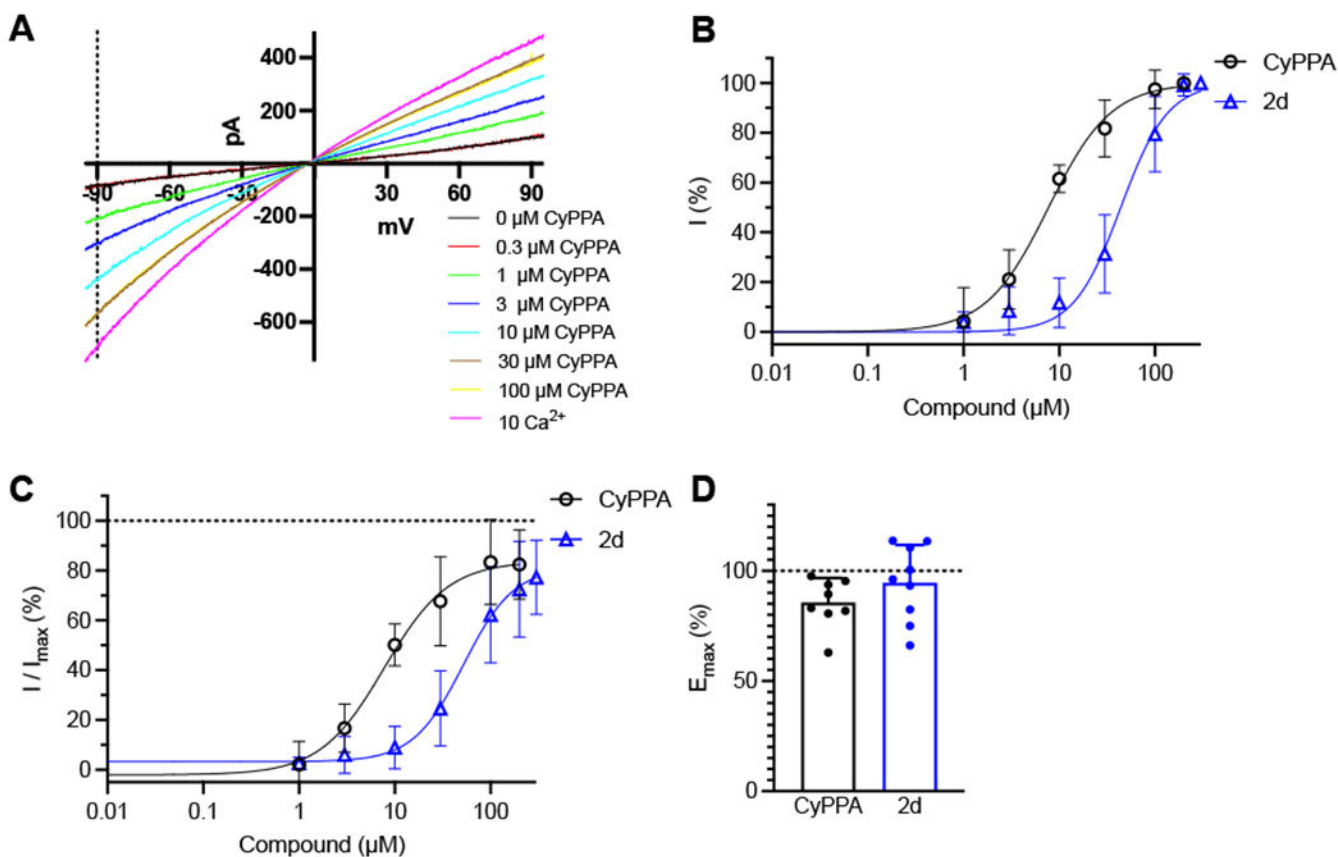


FIGURE 1. Modification of cyclohexane moiety in compound 2d did not improve potency on $K_{Ca2.2a}$ channels.

(A) Representative current traces of concentration-dependent potentiation by CyPPA of rat $K_{Ca2.2a}$ channels. (B) Concentration-dependent potentiation by **2d** and CyPPA of rat $K_{Ca2.2a}$ channels. (C) Responses to **2d** and CyPPA of rat $K_{Ca2.2a}$ channels were normalized to the maximal currents induced by 10 μ M Ca^{2+} . (D) E_{max} to **2d** and CyPPA of rat $K_{Ca2.2a}$ channels.

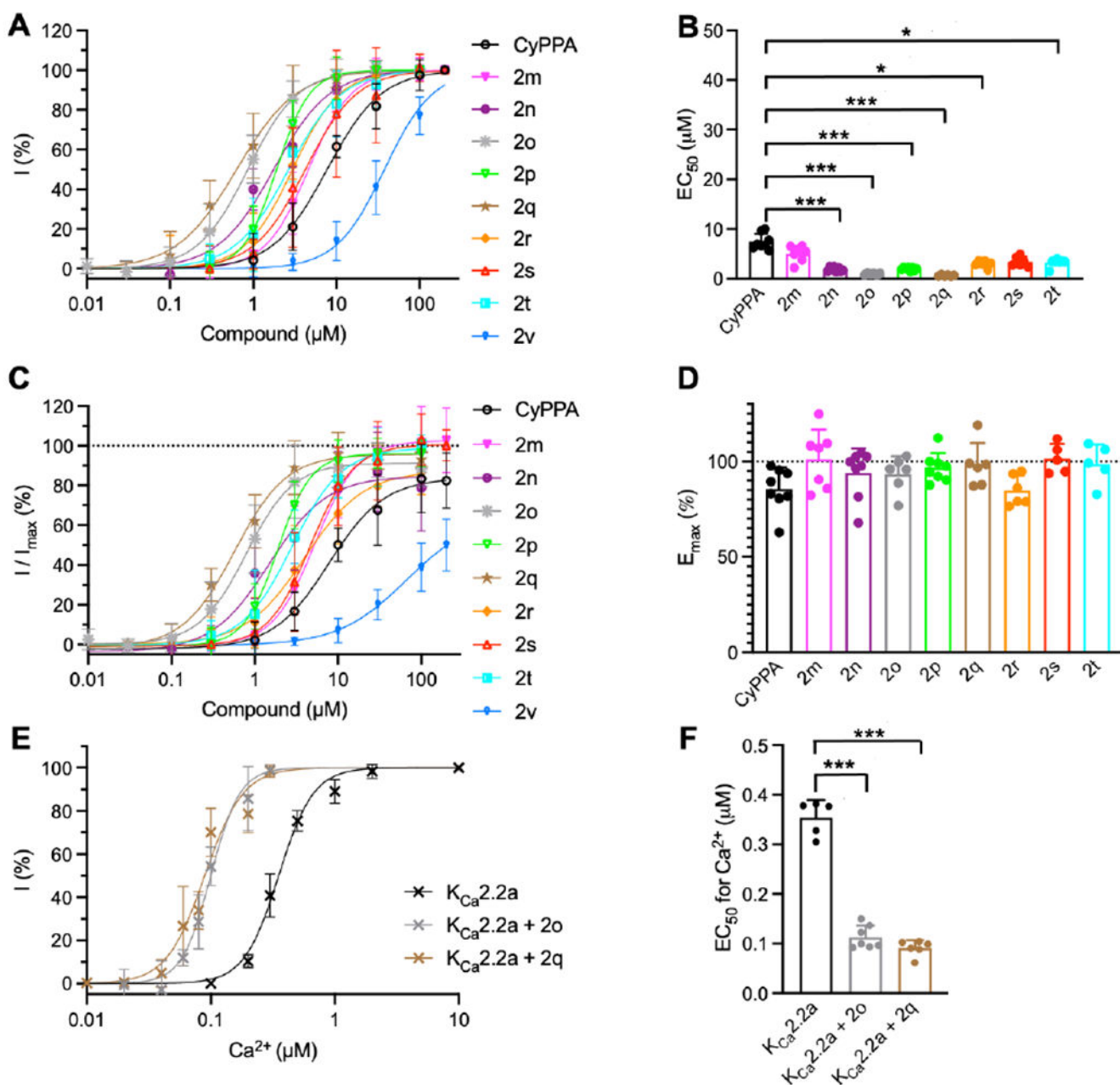


FIGURE 2. Changing from cyclohexane to substituted phenyl moiety in compounds 2n-r and 2t improved potency on $K_{Ca2.2a}$ channels.

(A) Potentiation by compounds with decorated phenyl moiety and CyPPA of rat $K_{Ca2.2a}$ channels. (B) EC_{50} values for potentiation by compounds with decorated phenyl moiety and CyPPA. (C) Responses to compounds of rat $K_{Ca2.2a}$ channels. The responses were normalized to the maximal currents induced by 10 μM Ca^{2+} . (D) E_{max} to compounds. * $P < 0.05$, *** $P < 0.001$. No asterisk means no statistical significance compared with CyPPA. (E) Effects of compounds 2o (10 μM) and 2q (10 μM) on the Ca^{2+} concentration-dependent activation of rat $K_{Ca2.2a}$ channels. (F) Increased apparent Ca^{2+} sensitivity of rat $K_{Ca2.2a}$ channels by compounds 2o (10 μM) and 2q (10 μM).

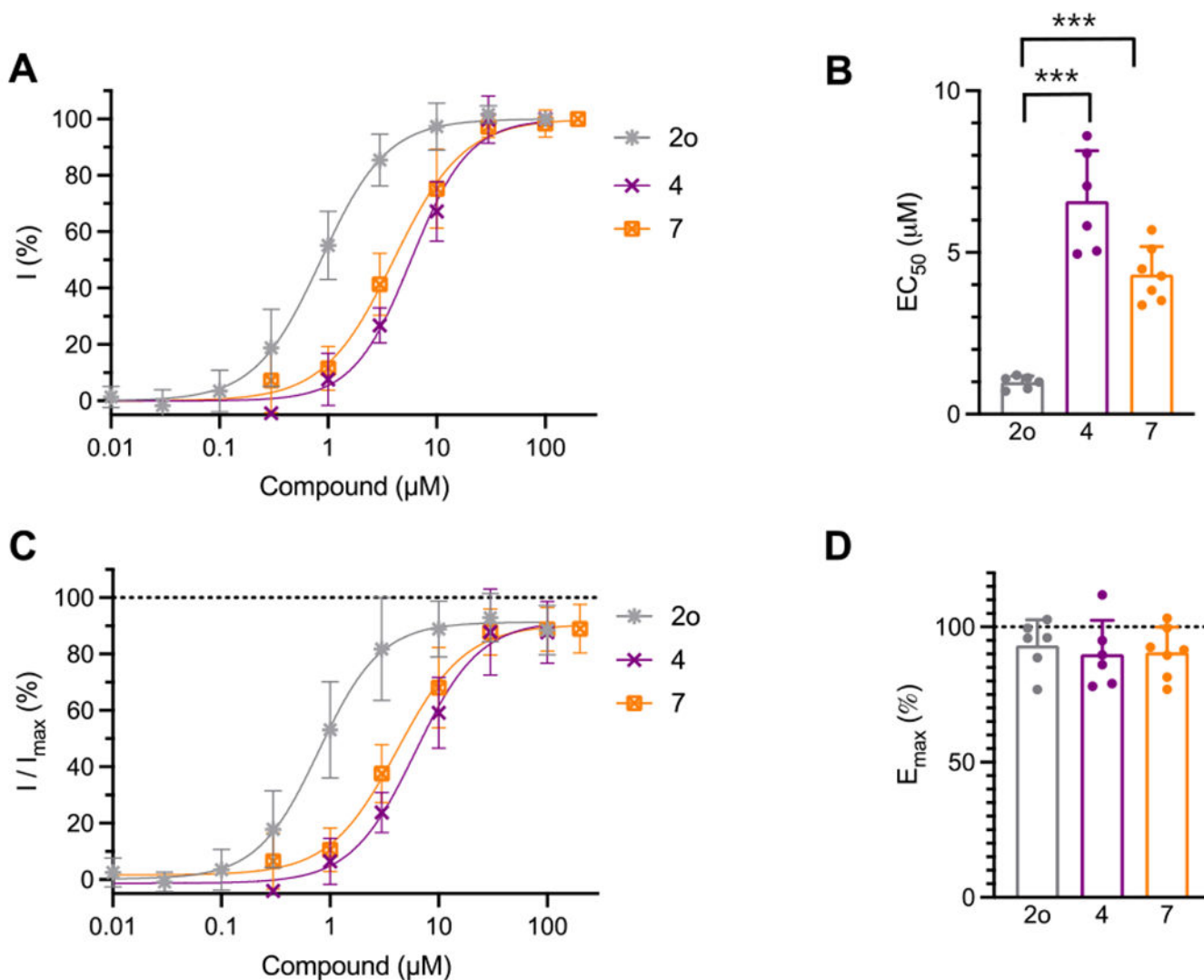


FIGURE 3. Modification of pyrimidine moiety in compounds 4 and 7 did not improve potency on $K_{Ca2.2a}$ channels.

(A) Potentiation by compounds with modified pyrimidine moiety of rat $K_{Ca2.2a}$ channels.

(B) EC_{50} values for potentiation by compounds with modified pyrimidine moiety. (C)

Responses to compounds of rat $K_{Ca2.2a}$ channels. The responses were normalized to the

maximal currents induced by 10 μM Ca^{2+} . (D) E_{max} to compounds. *** $P < 0.001$. No

asterisk means no statistical significance.

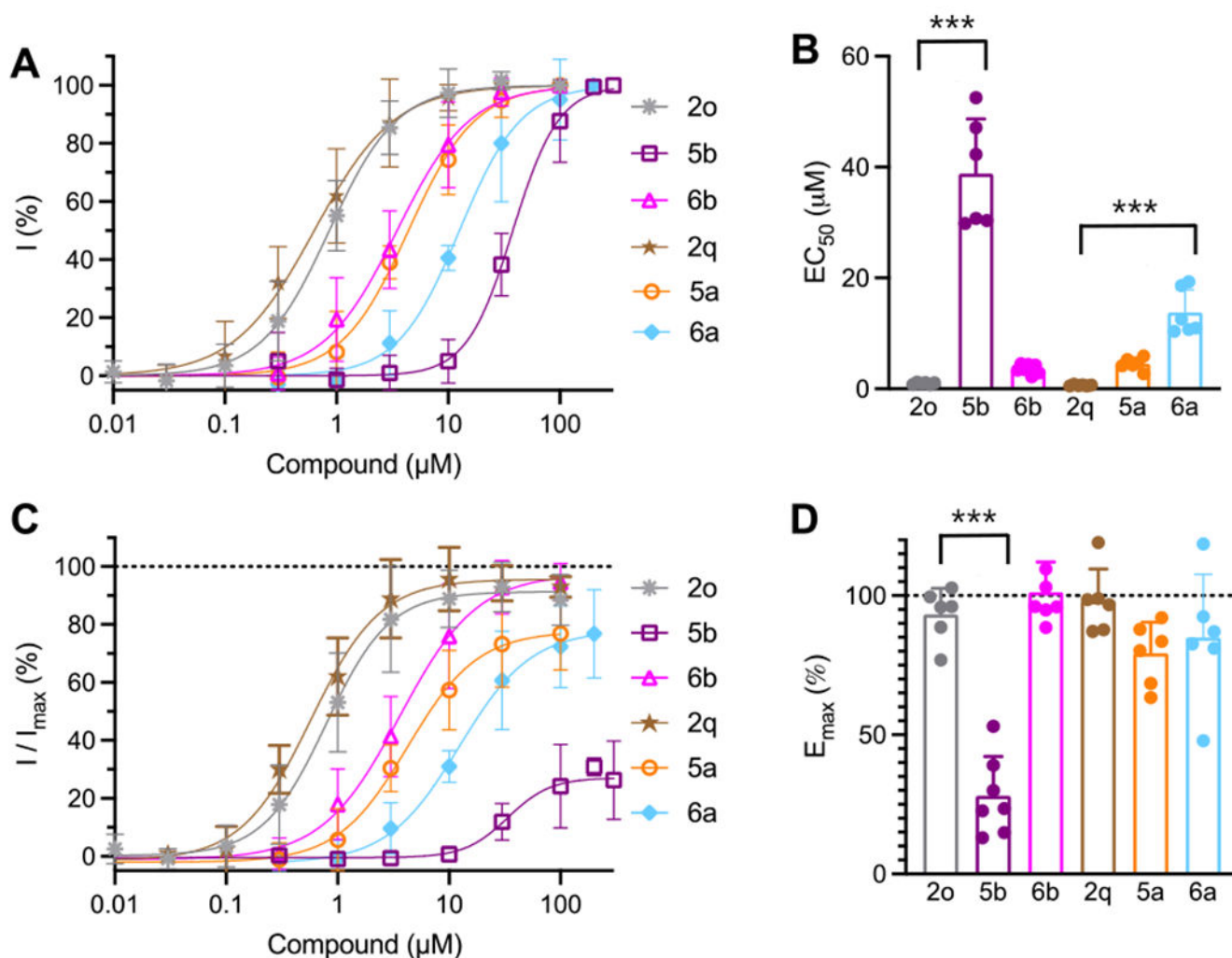


FIGURE 4. Modification of pyrazole moiety in compounds 5a-b and 6a-b did not improve potency on $K_{Ca2.2a}$ channels.

(A) Potentiation by compounds with modified pyrazole moiety of rat $K_{Ca2.2a}$ channels. (B) EC_{50} values for potentiation by compounds with modified pyrazole moiety. (C) Responses to compounds of rat $K_{Ca2.2a}$ channels. The responses were normalized to the maximal currents induced by 10μ M Ca^{2+} . (D) E_{max} to compounds. * $P < 0.05$, *** $P < 0.001$. No asterisk means no statistical significance compared with its respective template.

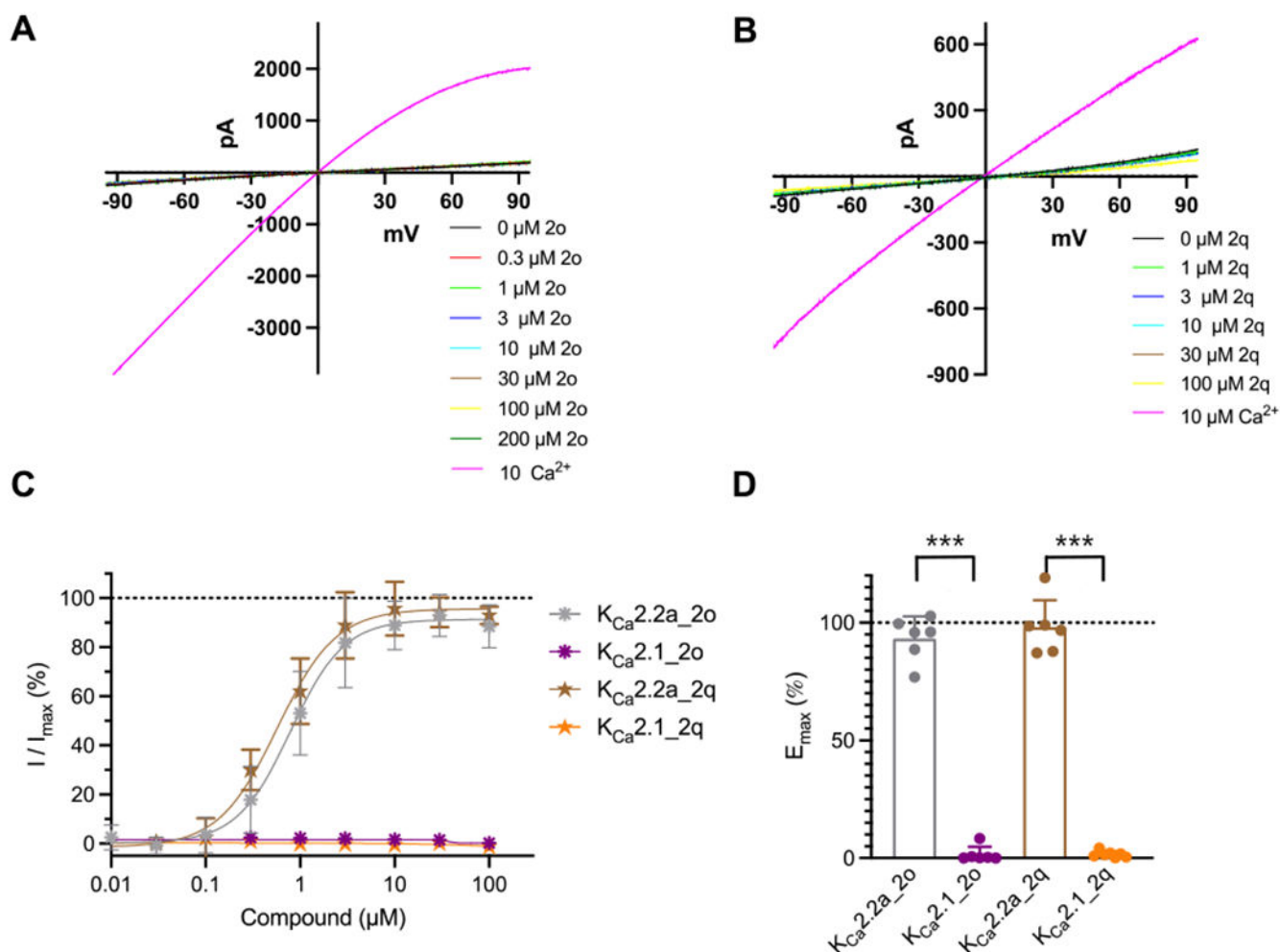


FIGURE 5. Subtype-selectivity towards $K_{Ca2.2a}$ over $K_{Ca2.1}$ channels.

(A) Lack of response to **2o** of human $K_{Ca2.1}$ channels. (B) Lack of response to **2q** of human $K_{Ca2.1}$ channels. (C) Responses to **2o** and **2q** of rat $K_{Ca2.2a}$ and human $K_{Ca2.1}$ channels. The responses were normalized to the maximal currents induced by $10 \mu\text{M Ca}^{2+}$. (D) E_{max} to **2o** and **2q** of rat $K_{Ca2.2a}$ and human $K_{Ca2.1}$ channels. *** $P < 0.001$.

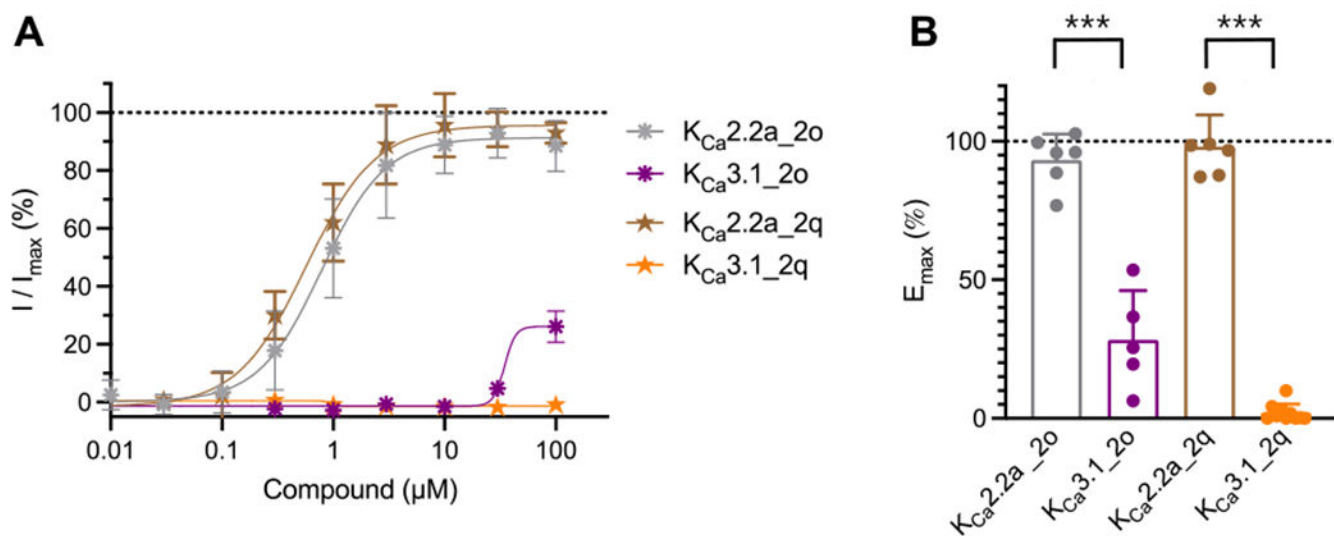


FIGURE 6. Subtype-selectivity towards $\text{K}_{\text{Ca}2.2a}$ over $\text{K}_{\text{Ca}3.1}$ channels.

(A) Responses to **2o** and **2q** of rat $\text{K}_{\text{Ca}2.2a}$ and human $\text{K}_{\text{Ca}3.1}$ channels. The responses were normalized to the maximal currents induced by $10 \mu\text{M}$ Ca^{2+} . (B) E_{max} to **2o** and **2q** of rat $\text{K}_{\text{Ca}2.2a}$ and human $\text{K}_{\text{Ca}3.1}$ channels. *** P < 0.001.

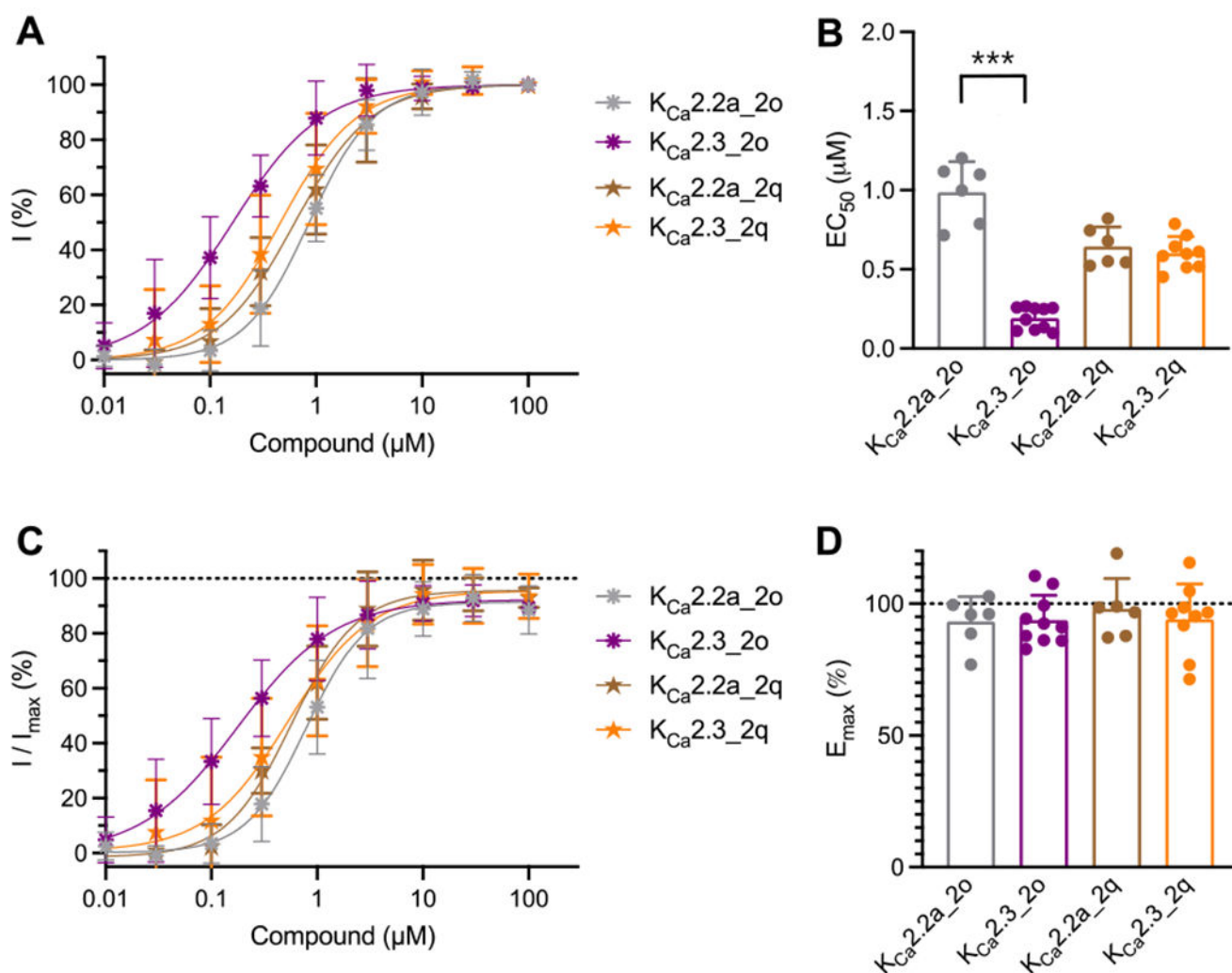


FIGURE 7. Activity on $K_{Ca}2.3$ channels.

(A) Potentiation by **2o** and **2q** of human $K_{Ca}2.3$ channels compared to rat $K_{Ca}2.2a$ channels.

(B) EC_{50} values for potentiation by **2o** and **2q** of human $K_{Ca}2.3$ channels compared to rat

$K_{Ca}2.2a$ channels. (C) Responses to **2o** and **2q** of human $K_{Ca}2.3$ channels compared to

rat $K_{Ca}2.2a$ channels.. The responses were normalized to the maximal currents induced by

$10 \mu M Ca^{2+}$. (D) E_{max} to **2o** and **2q** of human $K_{Ca}2.3$ channels compared to rat $K_{Ca}2.2a$

channels. *** $P < 0.001$. No asterisk means no statistical significance compared with rat

$K_{Ca}2.2a$ channel subtype.

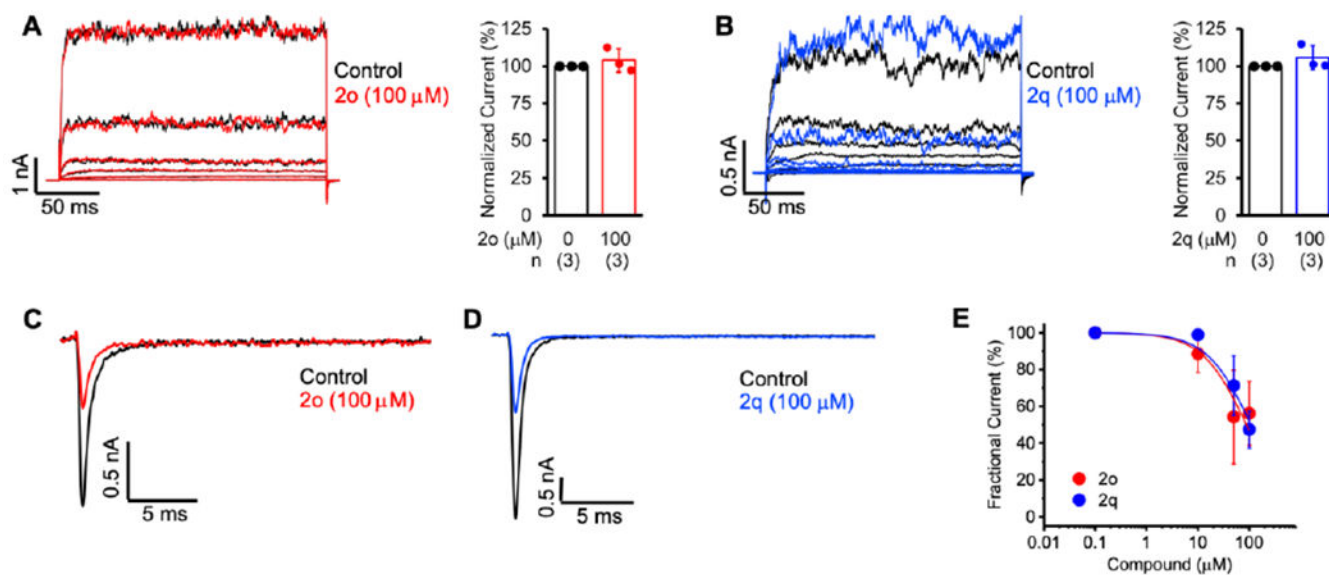


FIGURE 8. Effects of compounds **2o and **2q** on $K_{Ca}1.1$ and $Na_v1.2$ channels.**

(A) Representative human $K_{Ca}1.1$ currents in the absence or presence of **2o** (100 μM , left) and bar graph showing quantified current response by the +80 mV step (right). (B) Human $K_{Ca}1.1$ currents in the absence or presence of **2q** (100 μM). (C) Representative N1E-115 neuroblastoma mouse $Na_v1.2$ currents in the absence or presence of **2o** (100 μM). (D) Representative N1E-115 neuroblastoma mouse $Na_v1.2$ currents in the absence or presence of **2q** (100 μM). (E) Concentration-dependent inhibition of mouse $Na_v1.2$ currents by compounds **2o** (n = 5) and **2q** (n = 5).

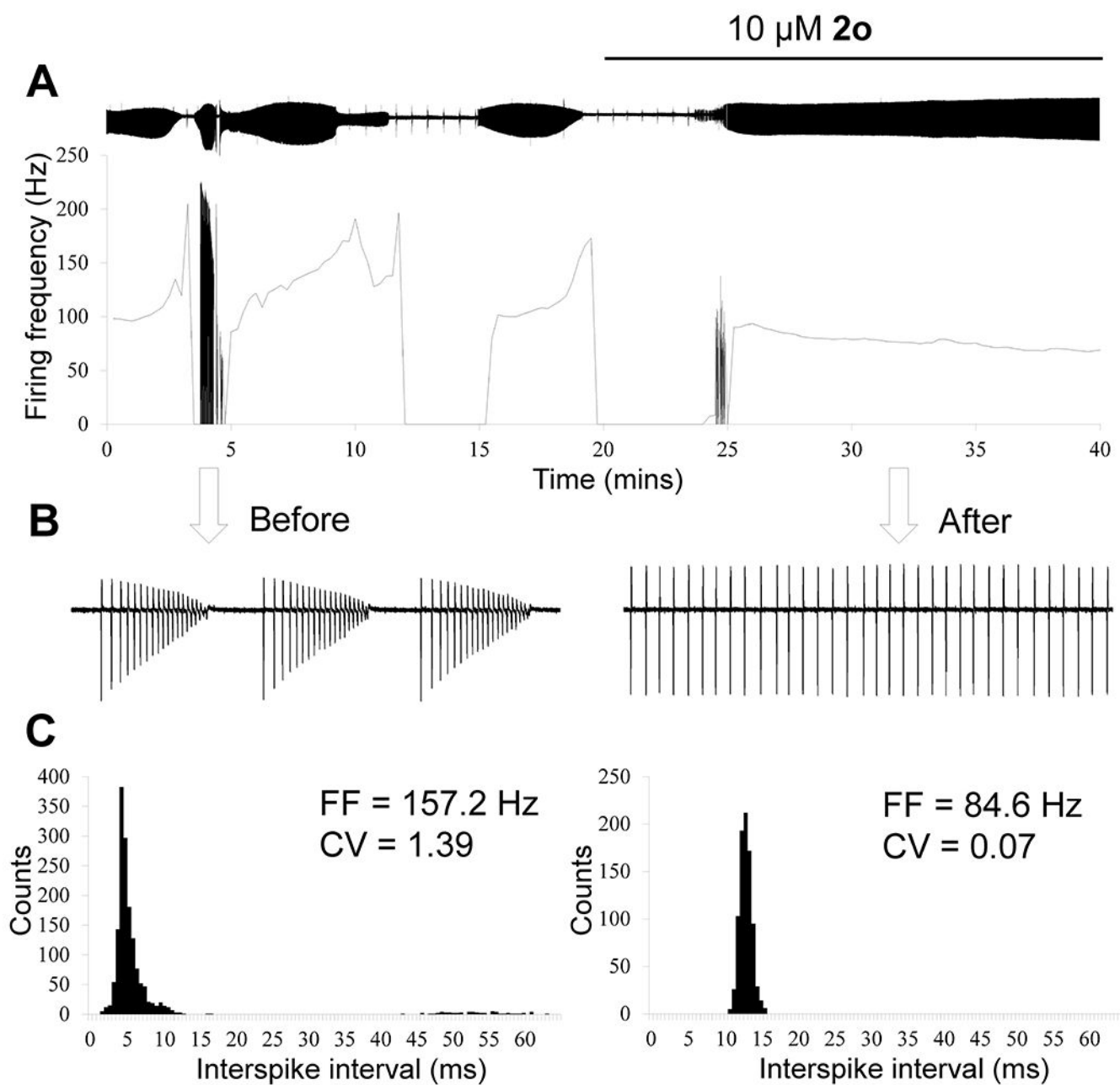


FIGURE 9. Subtype-selective $K_{Ca2.2a}/K_{Ca2.3}$ channel positive allosteric modulator **2o** converts bursting patterns into tonic activity of PC in acute cerebellar slices from 8-month-old SCA2-58Q mouse.

(A) Continuous 40-min recording of PC activity. The time of 10 μ M **2o** application is indicated by a horizontal bar above the recording. A plot of the running average of firing frequency is shown below the recording. (B) 390-ms fragments of PC activity recordings before the exposure to **2o** and 12 min after the exposure are shown on the expanded timescale. (C) The distributions of interspike intervals (ISI) before (left) and after (right) the exposure to **2o** were calculated from 10-s fragments of the recording shown in A. Average firing frequency (FF) for the analyzed fragment before **2o** application was 157.2 Hz, and the

CV of ISI in the analyzed fragment was 1.39. Average FF for the analyzed fragment after **20** exposure was 84.6 Hz, and the CV of ISI was 0.07.

Author Manuscript

Author Manuscript

Author Manuscript

Author Manuscript

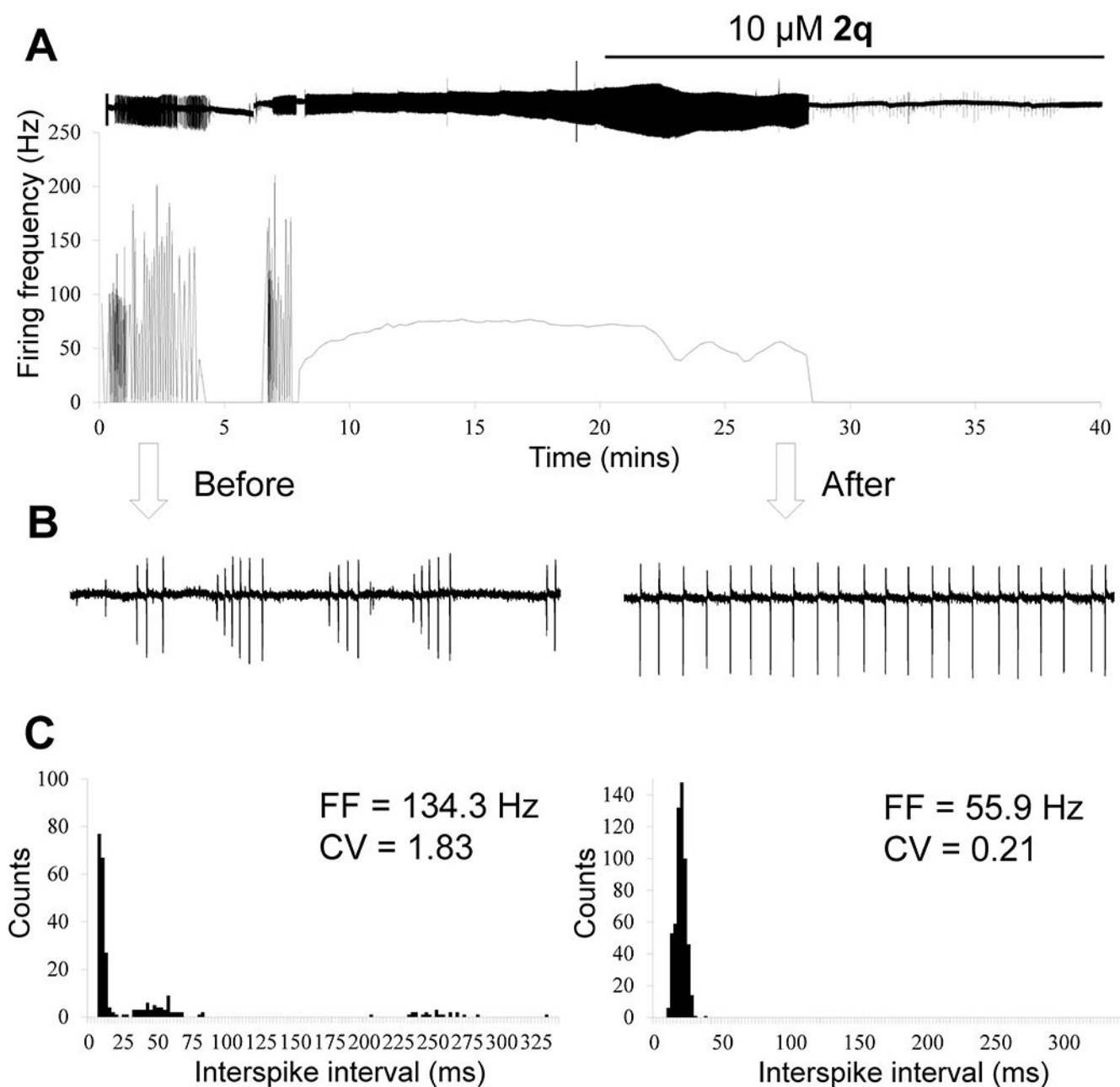


FIGURE 10. Subtype-selective $K_{Ca2.2a}/K_{Ca2.3}$ channel positive allosteric modulator **2q converts bursting patterns into tonic activity of PC and then into a silent mode in acute cerebellar slices from 8-month-old SCA2-58Q mouse.**

(A) Continuous 40-min recording of PC activity. The time of 10 μ M **2q** application is indicated by a horizontal bar above the recording. A plot of the running average of firing frequency is shown below the recording. (B) 390-ms fragments of PC activity recordings before the exposure to **2q** and 7 min after the exposure are shown on the expanded timescale. (C) The distributions of interspike intervals (ISI) before (left) and after (right) the exposure to **2q** were calculated from 10-s fragments of the recording shown in A. Average firing frequency (FF) for the analyzed fragment before **2q** application inside the bursts was

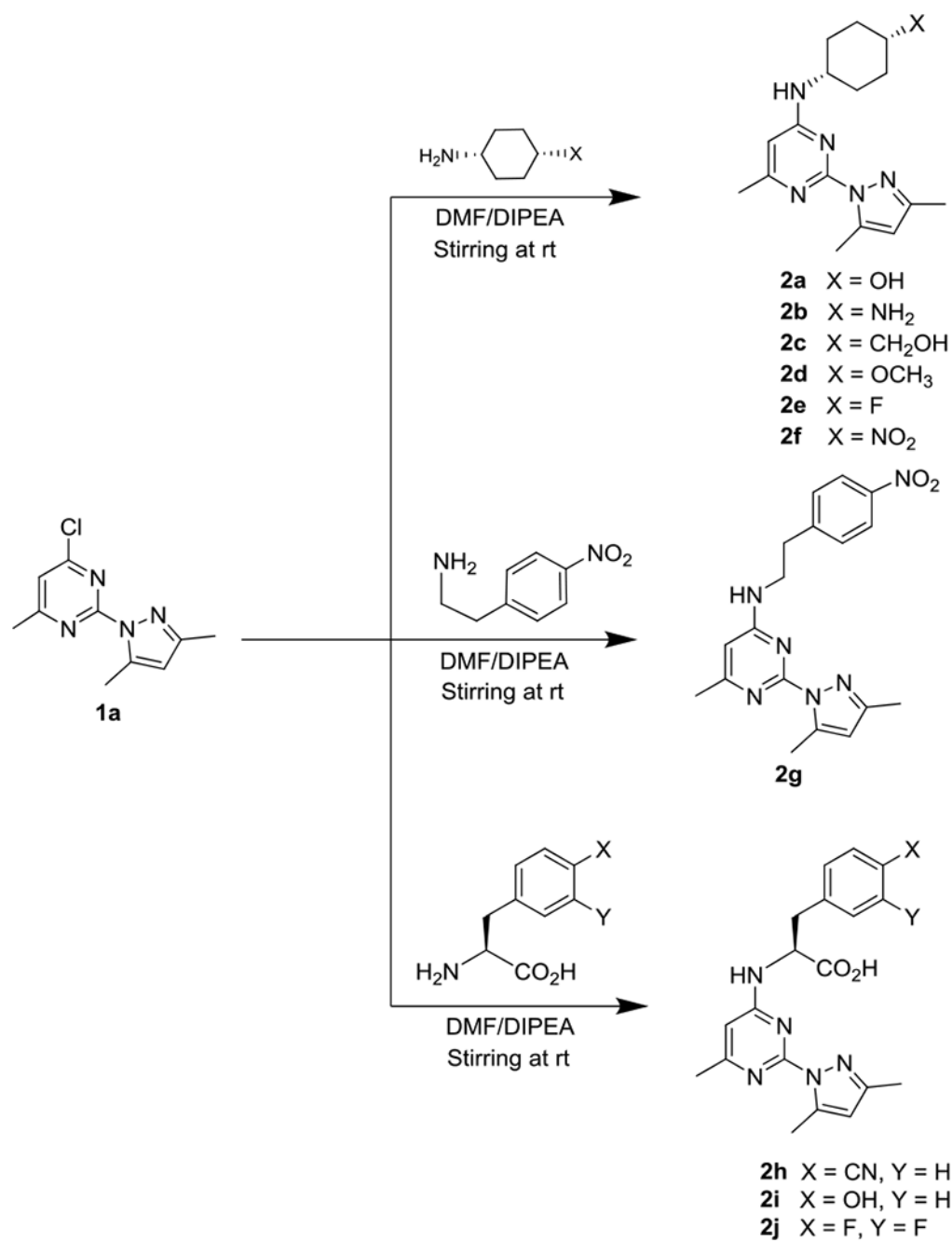
134.3 Hz, and the CV of ISI in the analyzed fragment was 1.83. Average FF for the analyzed fragment after **2q** exposure was 55.9 Hz, and the CV of ISI was 0.21.

Author Manuscript

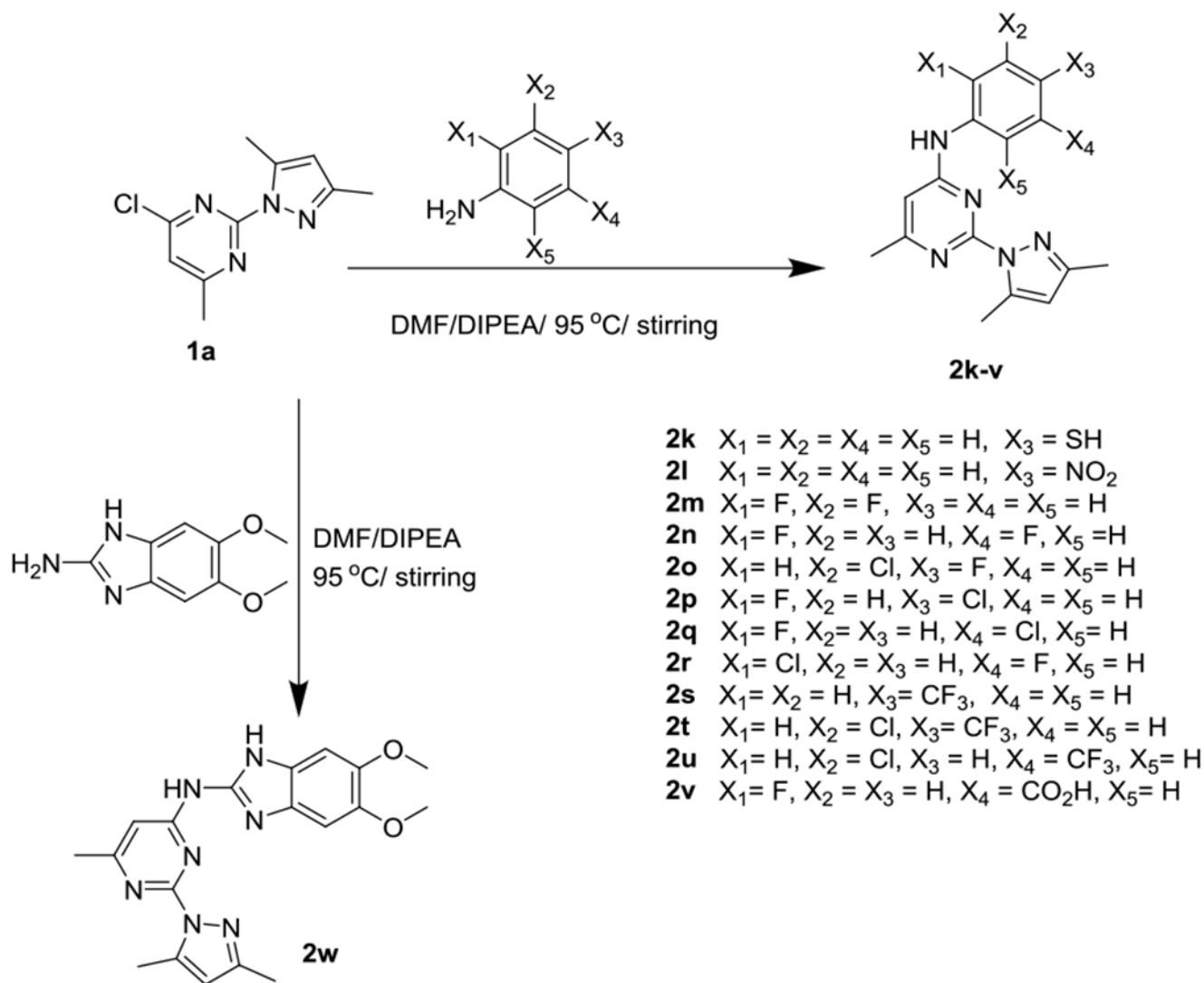
Author Manuscript

Author Manuscript

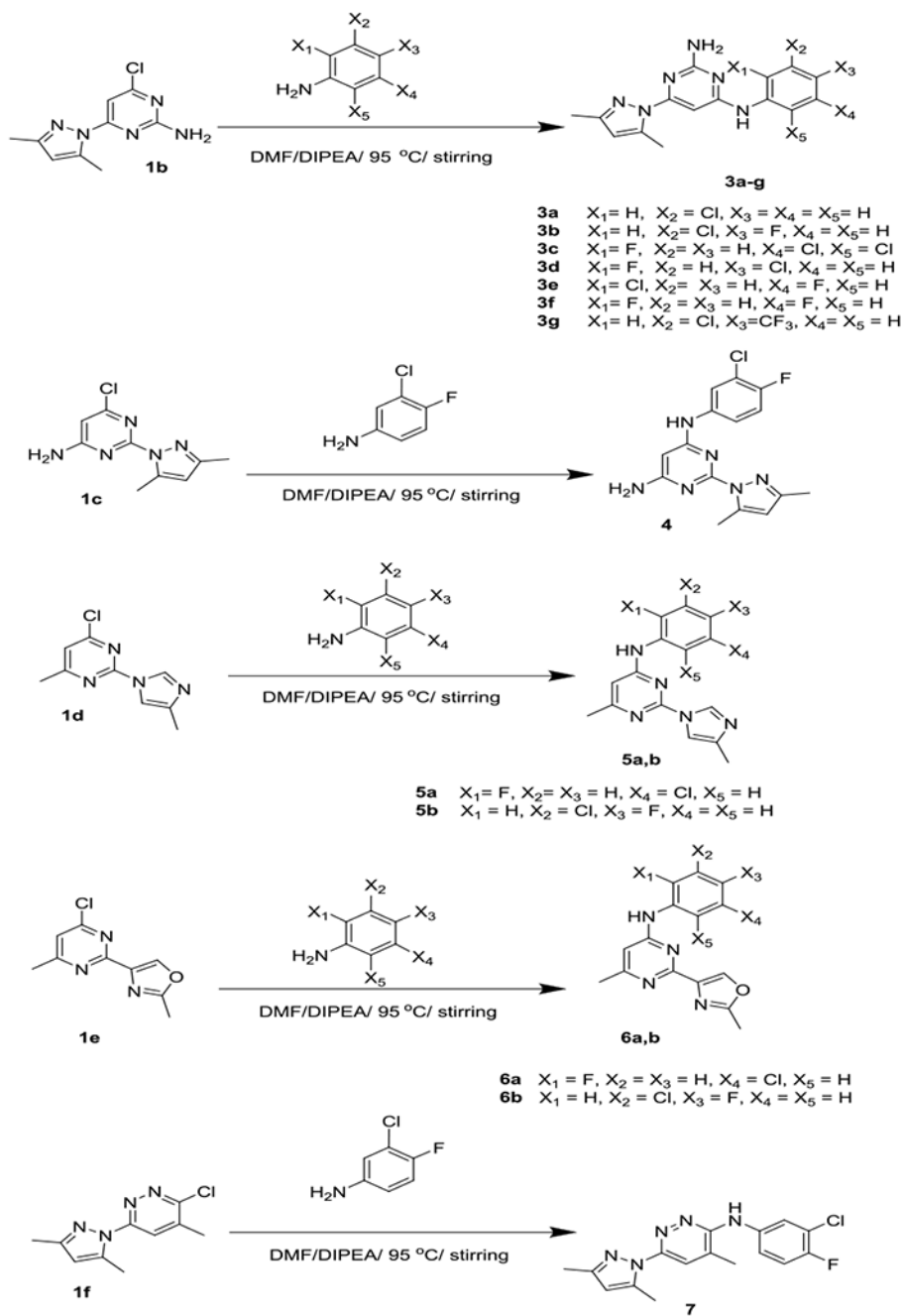
Author Manuscript



Scheme 1.
Synthesis of CyPPA analogs (**2a-j**).



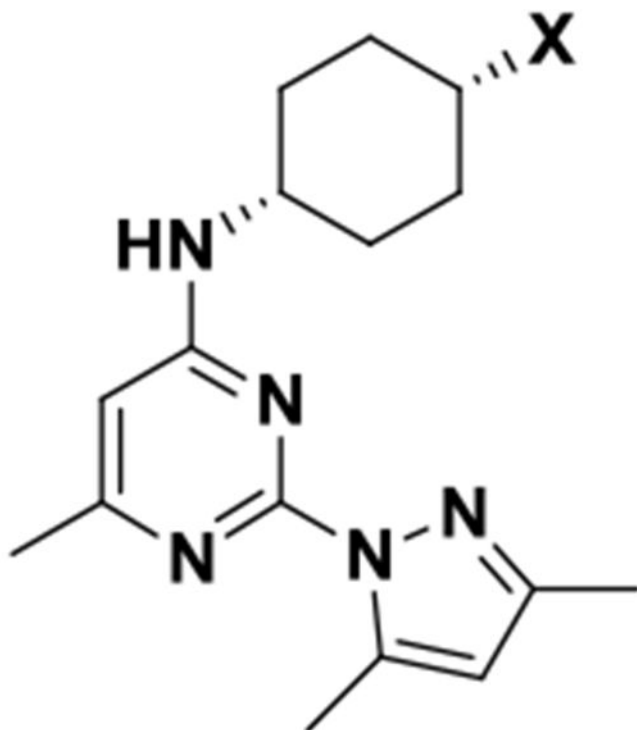
Scheme 2.
Synthesis of CyPPA analogs **2k-w**.



Scheme 3.
 Synthesis of CyPPA analogs (**3-7**).

Table 1.

The potency of compounds **2a-f** on potentiating rat $K_{Ca2.2a}$ channels compared to the parent template, CyPPA.



Compound	X	EC ₅₀ (μM)
2a	OH	> 100
2b	NH ₂	> 100
2c	CH ₂ OH	> 100
2d	OCH ₃	49.72 ± 11.3
2e	F	> 100
2f	NO ₂	> 100
CyPPA	H	7.48 ± 1.58

Table 2.

The potency of compounds **2g** and **2w** on potentiating rat $K_{Ca2.2a}$ channels compared to the parent template, CyPPA.

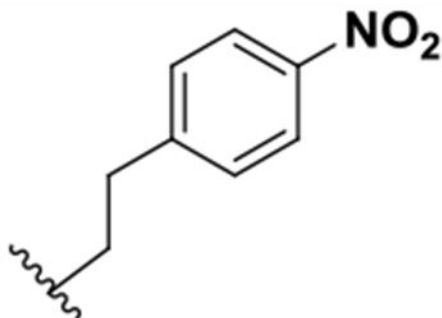
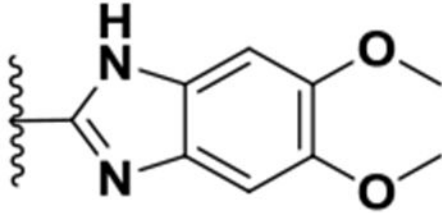
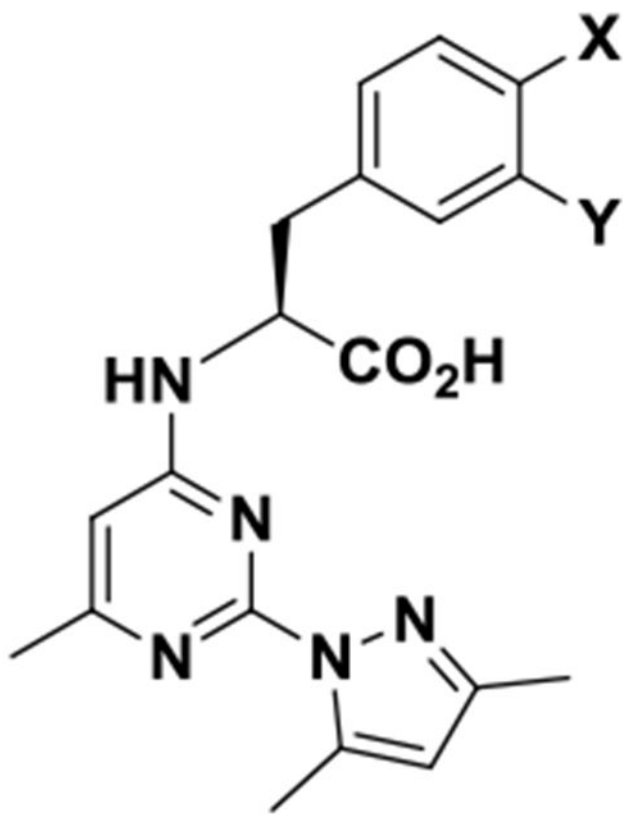
Compound	X	EC ₅₀ (μM)
2g		> 100
2w		> 100
CyPPA		7.48 ± 1.58

Table 3.

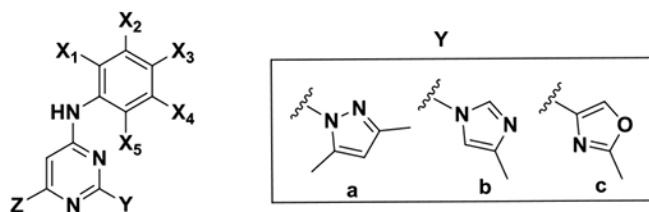
The potency of compounds **2h-j** on potentiating rat $K_{Ca2.2a}$ channels compared to the parent template, CyPPA.



Compound	X	Y	EC ₅₀ (μM)
2h	CN	H	> 100
2i	OH	H	> 100
2j	F	F	> 100
CyPPA			7.48 ± 1.58

Table 4.

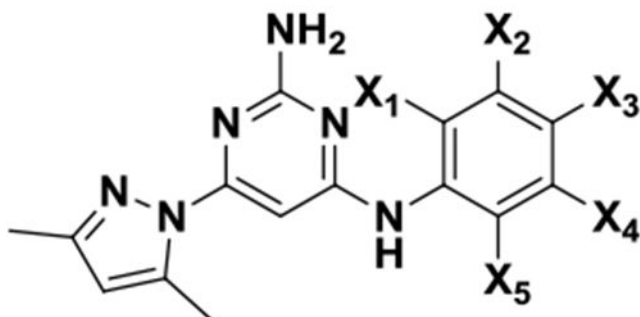
The potency of compounds **2k-v**, **4**, **5a-b**, and **6a-b** on potentiating rat $K_{Ca2.2a}$ channels compared to the parent template, CyPPA.



Compound	X ₁	X ₂	X ₃	X ₄	X ₅	Y	Z	EC ₅₀ (μM)
2k	H	H	SH	H	H	a	CH ₃	> 100
2l	H	H	NO ₂	H	H	a	CH ₃	> 100
2m	F	F	H	H	H	a	CH ₃	5.03 ± 1.06
2n	F	H	H	F	H	a	CH ₃	1.89 ± 0.44
2o	H	Cl	F	H	H	a	CH ₃	0.99 ± 0.19
2p	F	H	Cl	H	H	a	CH ₃	1.99 ± 0.31
2q	F	H	H	Cl	H	a	CH ₃	0.64 ± 0.12
2r	Cl	H	H	F	H	a	CH ₃	2.97 ± 0.67
2s	H	H	CF ₃	H	H	a	CH ₃	3.45 ± 1.00
2t	H	Cl	CF ₃	H	H	a	CH ₃	3.27 ± 0.79
2u	H	Cl	H	CF ₃	H	a	CH ₃	> 100
2v	F	H	H	CO ₂ H	H	a	CH ₃	> 30
4	H	Cl	F	H	H	a	NH ₂	6.59 ± 1.55
5a	F	H	H	Cl	H	b	CH ₃	4.51 ± 1.08
5b	H	Cl	F	H	H	b	CH ₃	38.81 ± 9.87
6a	F	H	H	Cl	H	c	CH ₃	13.77 ± 4.10
6b	H	Cl	F	H	H	c	CH ₃	3.59 ± 0.87
CyPPA								7.48 ± 1.58

Table 5.

The potency of compounds **3a-g** on potentiating rat $K_{Ca}2.2a$ channels compared to the parent template, CyPPA.



Compound	X ₁	X ₂	X ₃	X ₄	X ₅	EC ₅₀ (μM)
3a	H	Cl	H	H	H	> 100
3b	H	Cl	F	H	H	> 100
3c	F	H	H	Cl	H	> 100
3d	F	H	Cl	H	H	> 100
3e	Cl	H	H	F	H	> 100
3f	F	H	H	F	H	> 100
3g	H	Cl	CF ₃	H	H	> 100
CyPPA						7.48 ± 1.58